CONSTRUCTION MATERIALS CONSULTANTS, INC.

Laboratory Investigation of An Outdoor Suspended Concrete Slab Of An Underground Vault Adjacent To A Swimming Pool

Algonquin Pool
1614 Cypress Street
Louisville, KY 40210

July 8, 2020
CMC 0620128

Table Of Contents

Executive Summary 1
Introduction 3
Background Information 3
Purpose Of Present Investigation 3
Field Photographs 4
Core Locations 8
Methodologies 9
Petrographic Examinations (ASTM C 856) 9
Water-Soluble Chloride Contents From Potentiometric Titraiton (ASTM C 1218) 10
Samples 11
Photographs, Identification, Integrity, And Dimensions 11
End Surfaces 11
Cracking & Other Visible Distress, If Any 11
Embedded Items 11
Resonance 11
Petrographic Examinations 18
Lapped Cross Sections 18
Micrographs Of Lapped Cross Sections 22
Thin Sections 28
Micrographs Of Thin Sections 32
Coarse Aggregates In Concrete 52
Fine Aggregates In Concrete 52
Paste In Concrete 53
Air 54
Chlroide Profiles 54
Discussions 57
Cracking From Cyclic Freezing And Thawing Of Non-Air-Entrained Concrete 57
Cracking From Unsound Alkali-Silica Reactive Gravel Aggregates 57
Role Of Topping In Protecting Underlying Unsound Deteriorating Concrete Substrate 57
Carbonation-Induced Corrosion Of Reinforcing Steel In Concrete 58
Future Durability And Serviceability 58
References 58

EXECUTIVE SUMMARY

The present study involves detailed laboratory investigation of an outdoor swimming pool deck located in Louisville, KY. The deck represents a suspended top slab for an underground vault that houses equipment, filter, pump, etc. for the pool. The suspended deck slab was originally constructed back in 1955 as an 8-in. thick slab, which later received an additional 2-in. thick topping in 1991. The purpose of the present investigation is to evaluate the overall condition, durability, and future serviceability of the concrete substrate portion of the deck, which is in service since 1955.

Three composite cores were drilled from three locations around the pool deck and marked as Nos. 1 through 3. In all three cores, the topping, approximately $2^{1}/_{4}$ to 3 inches in thickness is present in sound, crack-free conditions but entirely de-bonded from the underlying concrete substrate. In two of the three cores (Nos. 1 and 3), the substrate concrete shows extensive cracking through the entire thickness of the recovered length of the substrate, whereas in the third core (No. 2) the entire substrate is completely fragmented into a bag full of rubbles. As a result, the relatively intact portions of concrete substrates in Core Nos. 1 and 3 were tested for the present study. Both samples were examined by detailed petrographic examinations according to the procedures of ASTM C 856 to evaluate the concrete conditions and evidence of any distress. Additionally, water-soluble chloride analyses were done from the top exposed wearing surface of the topping, the mid-depth location of concrete substrate, and the bottom end of concrete to evaluate the effectiveness of topping in preventing migration of chlorinated pool water into the slab along with potential migration of chloride into the slab from long-term exposure to chlorinated pool water and its potential role in causing any chloride-induced corrosion of reinforcing steel in the concrete.

Field photos of the underside of top suspended slab of the vault shows stalactite deposits from the cracks indicating extensive moisture migration through the top slab during the course of its service. Spalling of concrete at the underside of top suspended slab and exposure of corroded reinforcing steel at the spalled location indicates chloride and/or carbonation-induced corrosion of steel or corrosion from moisture infiltration through the slab during service.

Based on detailed petrographic examinations, the concretes in both Cores 1 and 3 are found to be compositionally similar and made using calcareous gravel coarse aggregates having nominal maximum sizes of 1 inch (25 mm) and containing limestone, dolomite, limestone having microcrystalline to cryptocrystalline silica or chert inclusions, dolomitic chert, fossiliferous limestone (biosparite), and siliceous limestone. Coarse aggregate particles are variably dense, variably porous, and variably colored from light to dark gray, brown, red, and other color tones that are characteristic of gravels. Particles are equidimensional to elongated, sub-rounded to well-rounded, unaltered, many show dark weathering and/or reaction rims, and mostly uncracked except the ones along the paths of cracks. Coarse aggregate particles are well-graded and well-distributed. Many limestone and dolomite particles having microcrystalline silica or chert inclusions show potential reactivity to cement alkalis in the presence of moisture, which is evidenced as dark reaction rims, cracks from reactive particles to paste, and occasional alkali-silica reaction gels inside such cracks. Coarse aggregate particles have been potentially unsound due to such alkali-silica reactions during their service in the concrete, and contributed to the extensive cracking seen through the entire depths of Cores 1 and 3.

Fine aggregates are compositionally similar natural siliceous-calcareous sands having nominal maximum sizes of $^{3}/_{8}$ in. (9.5 mm), where siliceous component contains quartz, quartzite, feldspar, chert, granite, sandstone, quartz siltstone and shale, and, calcareous component contains limestone and dolomite of various types mentioned in the calcareous gravel coarse aggregate particles. Particles are variably colored, rounded to subangular, dense, hard, equidimensional to elongated, unaltered, uncoated, and mostly uncracked except the ones along the paths of cracks. Fine aggregate particles are well-graded and well-distributed. There is no evidence of alkali-aggregate reaction of fine aggregate particles although such reaction is possible for many chert particles found in fine aggregate. Fine aggregate particles have been sound during their service in the concrete and did not contribute to the cracking of slab.

Pastes are moderately dense, medium gray, uniform in color throughout the depth of concrete. Freshly fractured surfaces has subvitreous lusters and subconchoidal textures. Residual and relict Portland cement particles are present and estimated to constitute 8 to 10 percent of the paste volumes. Besides Portland cement, no other pozzolanic or cementitious materials are found. Hydration of Portland cement is normal in the interior bodies. The textural and compositional features of the pastes are indicative of Portland cement contents estimated to be 6 to $6^{1}/_{2}$ bags per cubic yard, and, water-cement ratios (*w/c*) estimated to be 0.40 to 0.45 in the interior bodies of concrete. Carbonation is 1 to 2 mm from topping surface but sporadic throughout the interior of concrete. Aggregate-paste bonds are moderately tight to weak. Extensive microcracking is present in both cores that are judged to be primarily from freezing of concrete at critically saturated conditions, and secondarily from alkali-silica aggregate reactions of some reactive gravels.

Concrete in both Cores 1 and 3 are non-air-entrained having air contents estimated to be less than 1 percent.

Water-soluble chloride contents are determined from potentiometric titration according to the procedures of ASTM C 1218. Results showed 0.3 percent chloride by mass of cement in the topping in Cores 1 and 3, and, similar 0.3 percent chloride at the bottom end of Core 1, but no detectable chloride at mid-depth locations of either core, or at the bottom end of Core 3. Chloride contents are indicative of effectiveness of topping in prevention of migration of chloride into the concrete except for the chlorides already in the concrete from prior migrations during service of slab from 1955 to 1991.

The non-air-entrained nature of concrete and its exposure to an outdoor environment of cyclic freezing and thawing, and intermittent exposure of water from splashing of pool water have developed an ideal environment for cracking of a non-air-entrained concrete slab around the pool during freezing at critically saturated conditions. The extensive network of cracks oriented parallel to the exposed surface of concrete and extended through the entire depth of slab in both Cores 1 and 2 are the classic testaments of such freezing-induced deterioration of the slab especially due to its proximity to the pool water.

Cracks formed from cyclic freezing and thawing have opened up channels for migration of moisture deep inside the concrete. The presence of moisture, along with high alkalis from Portland cement used during mid-20th century, and potentially alkali-silica reactive chert component found in many limestone gravel particles have developed another ideal scenario for distress – alkali-silica reaction. Many reactive cherty limestone and dolomitic chert gravel coarse aggregate particles showed dark reaction rims, cracks extending from reactive gravels to paste, and alkali-silica reaction products inside the cracks – the three tell-tale signatures of distress due to alkali-silica aggregate reactions.

Alkali-silica reaction, however, is found to have played a subordinate role compared to freezing for development of most of the cracks seen in the concrete. It is the freezing-related cracks that have opened up pathways for migration of moisture deep inside the slab to promote alkali-silica reactions. Cracks from alkali-silica reaction have intensified the overall frequency of cracking, no doubt, but the overall surface-parallel orientation of cracks through the entire thickness of slab were most likely formed due to cyclic freezing and thawing of a non-air-entrained concrete at critically saturated conditions.

Unlike extensive through-depth cracking in the concrete substrate, the 2-in. thick topping placed in 1991 is free of any cracks and present in sound and serviceable condition. Most of the distress in concrete slab i.e. freezing-related through-depth cracking is judged to have formed during the service period of 1955 through 1991.

However, topping is not bonded to the underlying deteriorated concrete. In all three cores, the topping was completely de-bonded from the spalled concrete surfaces where the concrete surface was spalled due to freezing-related cracking. Topping was applied on concrete that contained many surface-parallel cracks that prevented development of a good bond to the newly applied topping.

Spalling of the underside of concrete in the suspended top slab of vault and exposed corroded steel reinforcement found in the field photos of underside of the top slab are distresses judged to be due to carbonation-induced corrosion of steel reinforcement situated near the formed bottom end of the top slab. This is evidenced from beige discoloration of concrete found at the bottom end of Core 1, in the fragmented bottom chunk in Core 2, and at the bottom end of Core 3 – all three cores showed such beige discoloration of paste due to carbonation of the underside surface of top slab from carbon dioxide in the ambient air of the vault. Corrosion of steel and associated reddish-brown corrosion products are observed in all three cores situated within this carbonated zone at the underside of top slab. Besides, water-soluble chloride analyses of concrete showed negligible chloride at the bottom end of Core 3 (except at the bottom of Core 1 which showed detectable chloride probably introduced from the pool water during service, probably prior to the installation of topping). The observed corrosion of steel at the underside and associated spalling probably occurred due to de-passivation of the protective oxide films around steel by reduction in inherent alkalinity of concrete by atmospheric carbonation. Moisture infiltration through preexisting cracks have also contributed to steel corrosion.

In summary, based on detailed petrographic examinations and chloride analyses of cores from around the pool deck, the observed deck slab, which represents the top suspended slab of adjacent underground vault is found to be present in poor, deteriorated condition from extensive through-depth cracking in two of the three cores to complete fragmentation of concrete in the third core. The topping in all three cores are present in sound and serviceable condition, however, with barely any bond to the underlying concrete substrate. Based on extensive cracking and fragmentation, future serviceability of the concrete substrate is judged to be poor, which is preferable to be replaced for long-term durability and serviceability of the pool deck.

INTRODUCTION

Reported herein are the results of laboratory studies of two composite cores consisting of a topping and a substrate concrete from an outdoor pool deck located in Louisville, KY. The pool deck is also a suspended slab for an adjacent vault that houses equipment and accessories for the pool. The purpose of this investigation is to evaluate the existing condition of the suspended slab since its installation back in 1955, which was followed by installation of the topping in 1991.

BACKGROUND INFORMATION

Figures 1 through 5 show: (a) the Algonquin Pool located in Louisville, KY (Figure 1), (b) the outdoor deck around the pool from where core samples for this study were collected (Figure 1), (c) the adjacent underground vault that houses various equipment, pump, filter, etc. of the pool (Figure 2), (d) the underside of the suspended slab deck around the pool from looking inside the vault that shows cracking and stalactite deposits from the underside of top slab (Figure 3), (e) spalling of concrete and exposure of corrode steel from underside of the suspended slab, etc. (Figure 3), (f) the deck, the pool, the underground vault, and the distress of the suspended top slab (Figure 4), and (g) the locations of thee cores around the pool that were collected for this study (Figure 5).

The original concrete slab around the pool was constructed back in 1955, which was approximately 8 inches in thickness. The slab was exposed to the elements from pool water to air to cyclic freezing and thawing. A 2-in. thick topping was installed back in 1991, a means to protect the existing concrete slab and extend its serviceability. The underground vault adjacent to the pool houses various equipment and accessories for the pool.

Occurrences of stalactite-type deposits from the underside of the top suspended slab are a testament that moisture migration has occurred through pre-existing cracks in the suspended slab during the course of its service.

PURPOSE OF PRESENT INVESTIGATION

Based on the background information, the purposes of the present investigation are to determine:

a. Compositions, qualities, and overall conditions of the concrete substrate portion of two (Nos. 1 and 3) of the three cores received where the concrete is present in relatively intact condition; and,
b. Chemical, mineralogical, and microstructural features of concrete to investigate future durability and serviceability of the concrete.

FIELD PHOTOGRAPHS

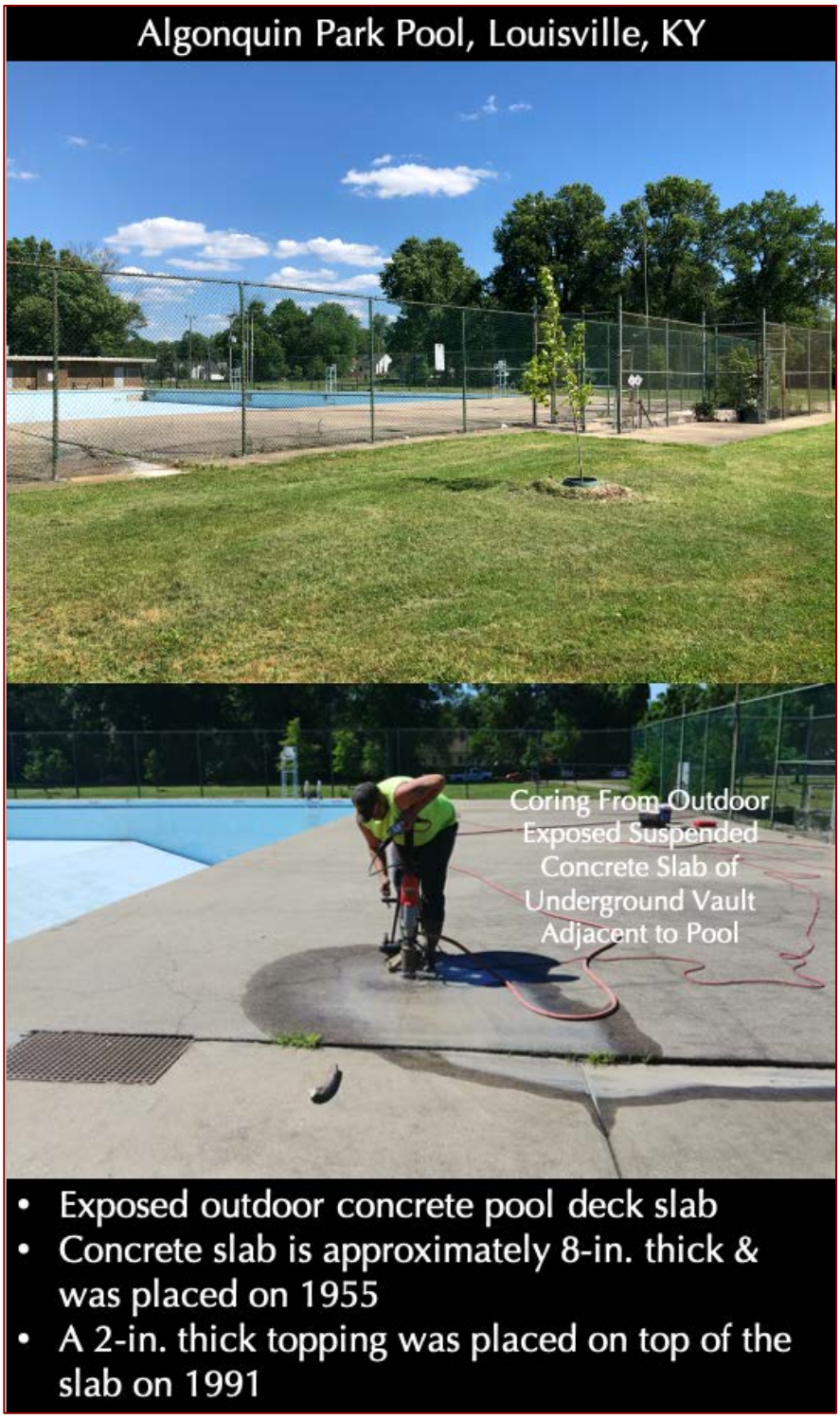

Figure 1: Top Photo - Algonquin Swimming Pool. Bottom Photo – Outdoor exposed concrete Deck around the pool, which also represents the suspended roofing slab for an underground vault that houses various pool equipment and accessories, e.g., pump, filter, and chlorine tanks.

Core samples for this study were collected from this pool-side slab as shown in the bottom photo.

The slab is reportedly 8 inches in thickness and was placed in 1955.

A 2-in. thick topping was placed on top of the structural concrete slab in 1991.

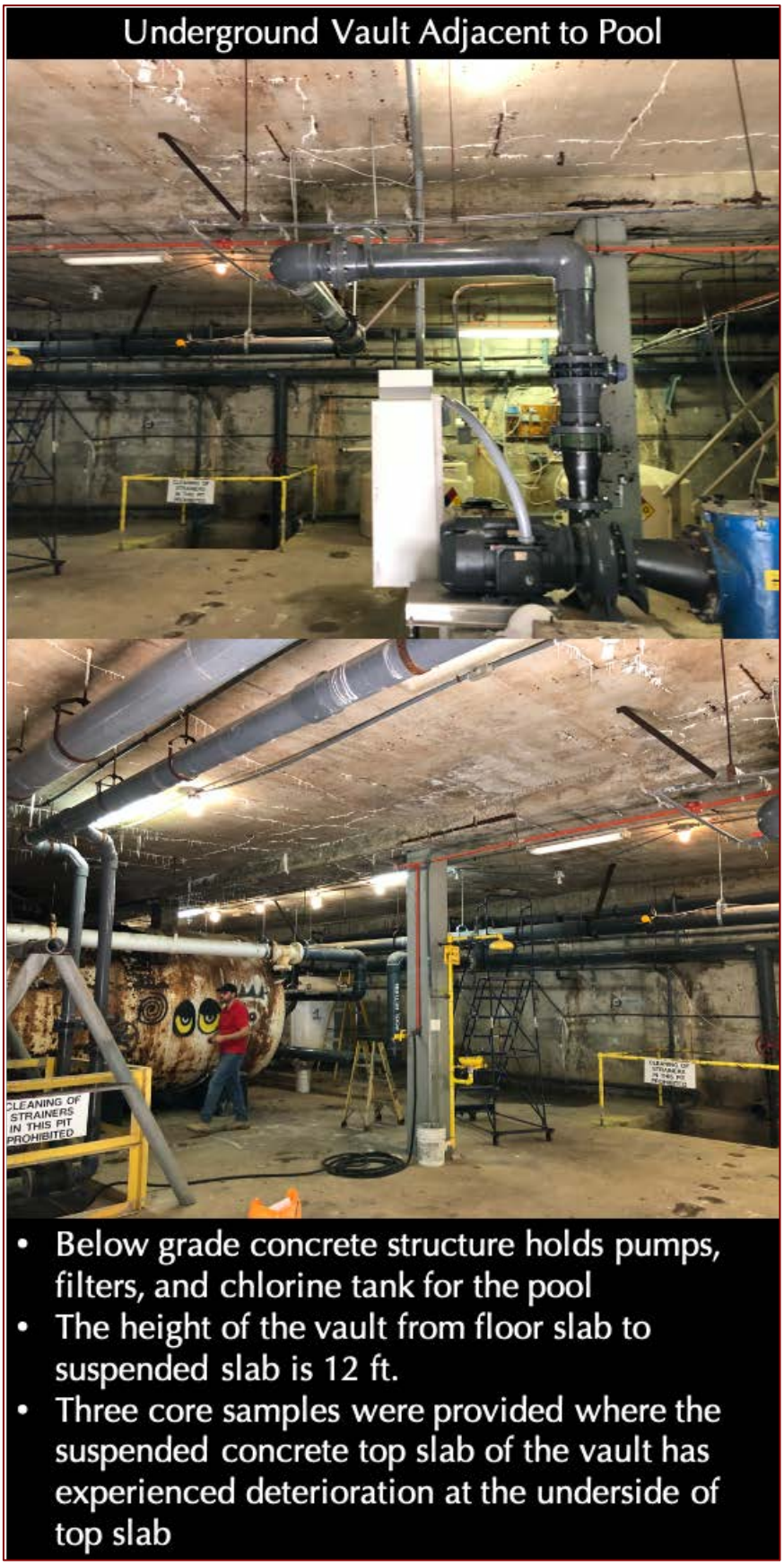

Figure 2: Underground vault adjacent to the pool that houses various equipment and accessories for the pool. Notice the underside of top suspended slab of the vault that has many stalactite deposits hanging from the visible cracks due to migration of moisture through pre-existing cracks in the pool slab deck leaching soluble components of the concrete and eventually precipitating as stalactite deposits from the roof.

Figure 3: Close-up of the underside of the top suspended slab of underground vault that shows white stalactite deposits from pre-existing cracks in the top photo, and spalling of concrete due to corrosion of reinforcing steel exposing the corroded steel in the bottom photo.

Figure 4: The top left photo shows the exposed outdoor suspended pool deck slab that has a 2-in. thick topping placed in 1991 above an 8-in. thick structural concrete slab placed in 1955. The top right photo shows the pool adjacent to the suspended deck slab above an underground vault system. Bottom two photos show the underground vault that houses various equipment and accessories for the pool.

CORE LOCATIONS

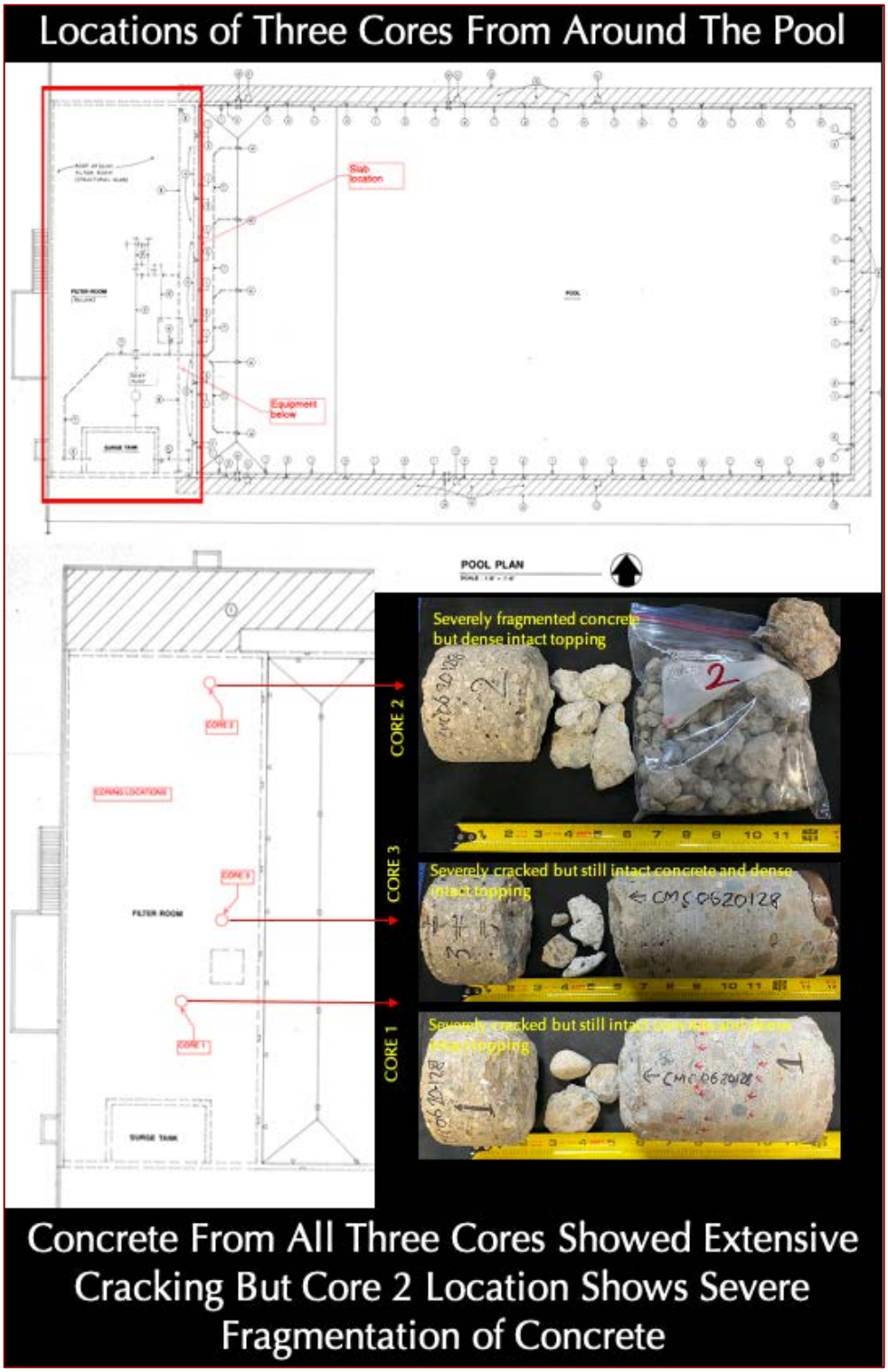

Figure 5: Schematic diagram showing the locations of three cores collected for this study.

Core 1 was received in broken condition where the 2-in. thick topping was entirely separated from the concrete substrate. The concrete showed extensive through-depth cracks oriented parallel to the top surface.

Core 2 was received in mostly fragmented condition for the concrete substrate, where, however, the topping is still dense and intact but entirely separated from rubble concrete substrate.

Core 3 was received in broken condition as well where concrete substrate showed most intact condition (though later found to have extensive through-depth microcracking).

Topping in all three cores are approximately 2 in. in thickness and completely de-bonded from concrete substrate.

Concrete substrate in all three cores show extensive through-depth cracking in Cores 1 and 3 to complete fragmentation in Core 2.

METHODOLOGIES

PETROGRAPHIC EXAMINATIONS (ASTM C 856)

The core samples were examined by petrographic examinations by following the methods of ASTM C 856 "Standard Practice for Petrographic Examination of Hardened Concrete." Details of petrographic examinations and sample preparation are described in Jana (2006). The steps of petrographic examinations include (Jana 2006):

i. Visual examinations of samples, as received;
ii. Low-power stereo microscopical examinations of as-received, saw-cut and freshly fractured sections, and lapped cross sections of samples for evaluation of textures, and composition;
iii. Low-power stereo microscopical examinations of air contents and air-void systems of concretes in the samples;
iv. Examinations of oil immersion mounts in a petrographic microscope for mineralogical compositions of specific areas of interest;
v. Examinations of fluorescent dye-mixed (to highlight open spaces, cracks, etc.) epoxy-impregnated lapped cross sections and large area (50 mm × 75 mm) thin sections in a petrographic microscope for detailed compositional and microstructural analyses;
vi. Photographing samples, as received and at various stages of preparation with a digital camera and a flatbed scanner; and,
vii. Photomicrographs of lapped sections and thin sections of samples taken with stereomicroscope and petrographic microscope, respectively to provide detailed compositional and mineralogical information of concrete.

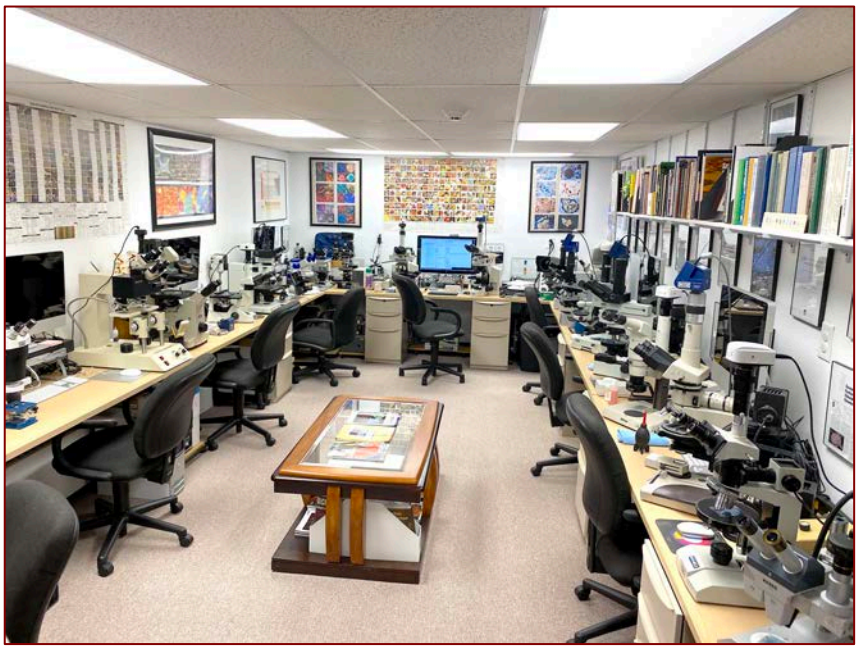

Figure 6: Optical microscopy laboratory in CMC that houses various stereo-microscopes, and petrographic microscopes used in this study.

The main purposes of optical microscopy are characterization of: (a) aggregates, e.g., type(s), chemical and mineralogical compositions, nominal maximum size, shape, angularity, grain-size distribution, soundness, alkali-aggregate reactivity, etc. (b) paste, e.g., compositions and microstructures to diagnose various type(s) of binder(s) used, (c) air, e.g., presence or absence of air entrainment, air content, etc., (d) alterations, e.g., lime leaching, carbonation, staining, etc. due to interactions with the environmental agents during service, and effects of such alterations on properties and performance; and (e) various chemical and/or physical deteriorations during service, including explanation of any visible cracking from various mechanisms. Portions selected from preliminary examinations for microscopy are sectioned, polished, and thin-sectioned (down to 25-30 micron thickness) preferably after encapsulating and impregnating with a fluorescent dye-mixed epoxy to improve the overall integrity of the sample during precision sectioning and grinding, and to highlight porous areas, voids, and cracks. Prepared sections are then examined in a high-power (up to 100X) Stereozoom microscope having reflected, transmitted, fluorescent light, and plane and crossed polarized-light facilities, and eventually in a high-power (up to 600X) petrographic microscope equipped with transmitted, reflected, polarized, and fluorescent-light facilities. Capturing high-resolution photomicrographs with these microscopes via digital microscope cameras with image analyses software are an integral part of documentations during petrographic examinations.

WATER-SOLUBLE CHLORIDE CONTENTS FROM POTENTIOMETRIC TITRAITON (ASTM C 1218)

The topping and concrete components of Cores 1 and 3 were selected for determination of chloride contents at the exposed surface of topping, at the mid-depth location of concrete, and at the bottom end of concrete. The purposes of such sample selection are: (a) to determine the effectiveness of topping in mitigating migration of chloride into the concrete since its installation in 1991, and, (b) determination of chloride levels present inside the concrete slab since its installation back in 1955, which might or might not have an influence on the observed corrosion of reinforcing steel in the concrete seen at the underside of suspended top slab of the vault.

Samples for chloride analyses were selected by trimming small pieces from each depth with a water-cooled diamond saw. Trimmed pieces were pulverized down to finer than 0.3 mm size. Approximately 10 grams of pulverized sample was thoroughly digested in 100 ml deionized water first in near-boiling temperature for 15 minutes with magnetic stirrer, followed by further room-temperature digestion for a period of 24 hours.

The digested sample solution was then filtered under vacuum, first through two 2.5-micron filter papers, followed by another filtration through two 0.2-micron filter papers to collect the filtrate. The filtrate thus obtained was diluted to a final volume of 200 ml in a volumetric flask. The filtrates thus prepared were used for potentiometric titration with a silver nitrate titrant *a la* ASTM C 1218 by using Metrohm 916 Ti-Touch titration apparatus with attached 814 Auto Sample Processor to determine the chloride contents. The instruments were calibrated with standard sodium chloride solutions for confirmation of known chloride contents in the blank solutions. The leftmost two instruments in the following Figure 7 set-up were used for the present study.

Figure 7: Set-ups for fully automated chloride analysis of concrete by potentiometric titration.

SAMPLES

PHOTOGRAPHS, IDENTIFICATION, INTEGRITY, AND DIMENSIONS

Figures 8 through 13, and Table 1 provide the overall dimensions and conditions of the cores received. Figures 14 through 17 show lapped cross sections of cores. ***Only the concrete components of Cores 1 and 3 were requested for the present study.***

Core ID	Diameter	Topping Length	Concrete Length	End Surfaces	Distress/Condition
#1	$3^5/_8$in. (95 mm)	$2^1/_4$ in. (55 mm)	Rubble+$5^1/_4$ in. (135 mm)	Exposed wearing surface of topping, relatively flat underside of topping completely de-bonded from underlying concrete, fractured surface of concrete at the top and formed surface of concrete at the bottom with extensive through-depth cracks in the concrete	Extensive through-depth cracking in concrete but no cracking in topping; intact condition of concrete despite cracking
#2	$3^5/_8$in. (95 mm)	3 in. (75 mm)	All Rubble	Exposed wearing surface of topping, relatively flat underside of topping completely de-bonded from underlying concrete, which has turned into a bag of rubbles	Concrete is extensively cracked to turn into a bag full of rubbles
#3	$3^5/_8$in. (95 mm))	$2^3/_8$ in. (60 mm)	Rubble+$7^1/_2$ in. (190 mm)	Exposed wearing surface of topping, relatively flat underside of topping completely de-bonded from underlying concrete, fractured surface of concrete at the top and fractured surface of concrete at the bottom with extensive through-depth cracks in the concrete that are visible only after fluorescent epoxy treatment	Extensive through-depth cracking in concrete visible after fluorescent epoxy treatment but no cracking in topping; intact condition of concrete despite cracking

Table 1: Overall dimensions and conditions of the grout cores received for laboratory examinations.

END SURFACES

End surfaces of topping and concrete components of cores are described in Table 1.

CRACKING & OTHER VISIBLE DISTRESS, IF ANY

Cracks are described in table 1 where the topping component shows no cracking whereas underlying concrete substrate showed extensive through-depth cracking to the point of compete fragmentation in Core 2.

EMBEDDED ITEMS

Core 1 has a No. 2 reinforcing steel at $2^3/_4$ in. depth from the formed base of concrete, which is corroded. Core 3 has a No. 5 reinforcing steel at the fractured base of concrete, which is corroded. Corrosion in both Cores 1 and 3 are found to be at the carbonated base of concrete. No wire mesh, fiber, or other embedded items are found.

RESONANCE

The cores have a dull resonance, when hammered.

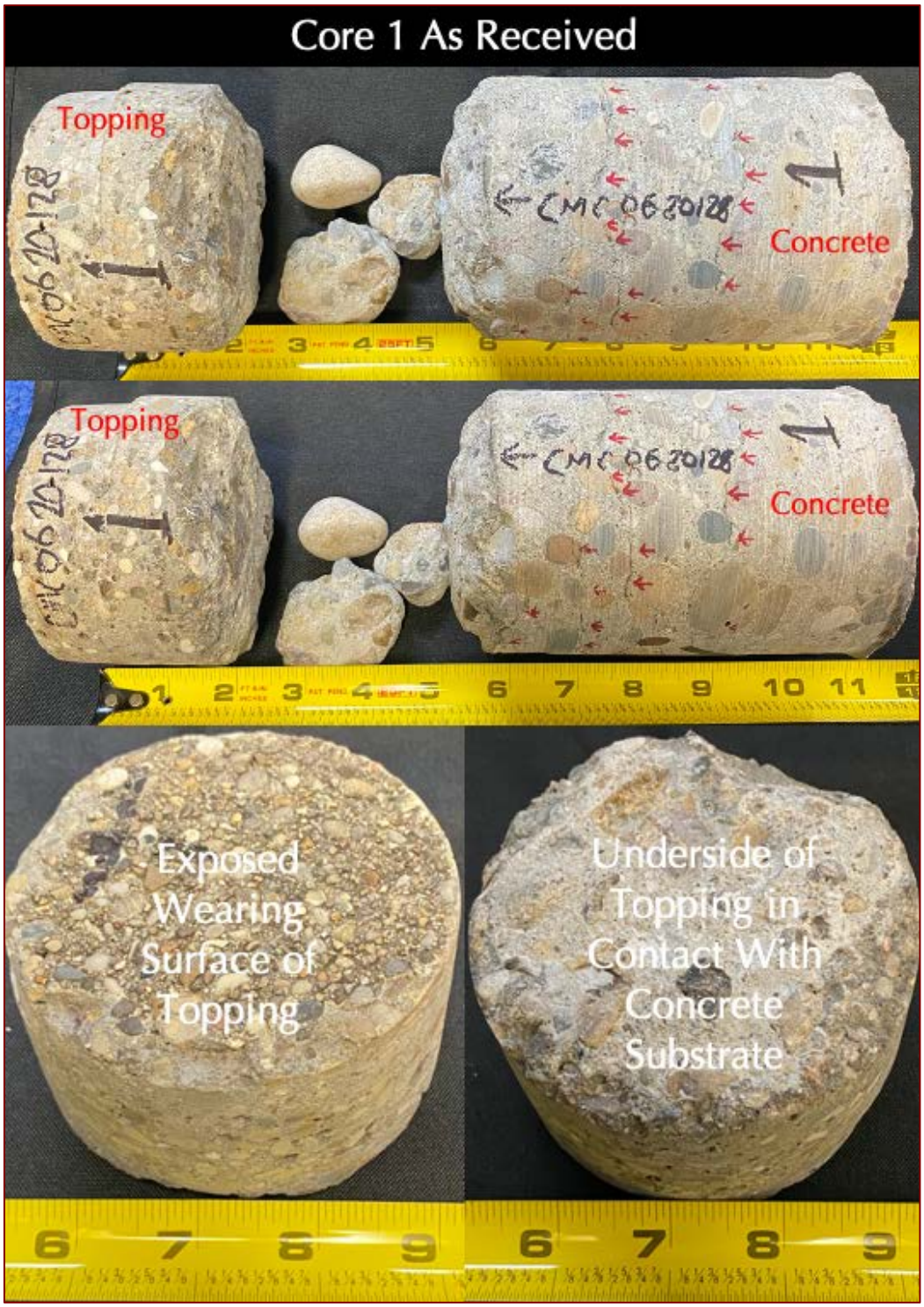

Figure 8: Core 1 as received showing:

(a) A 2-in. thick topping entirely detached from concrete substrate;

(b) Dense, sound, and well-consolidated nature of topping,

(c) A few rubbles of concrete between topping and fractured top surface of concrete;

(d) Extensive through-depth cracking in the concrete substrate that are oriented parallel to the top surface;

(e) Overall intact condition of concrete despite extensive cracking; and,

(f) Exposed weathered surface of topping and relatively flat underside of topping showing a more or less clean separation from the concrete substrate with no sign of a good bond between the two components.

Figure 9: Core 1 as received showing:

(a) Extensive through-depth cracking in the concrete substrate that are oriented parallel to the top surface; and,

(b) Overall intact condition of concrete despite extensive cracking.

Through-depth cracks are marked that have transected and circumscribed the aggregate particles.

Concrete shows the presence of gravel coarse aggregate particles that are well-graded and well-distributed.

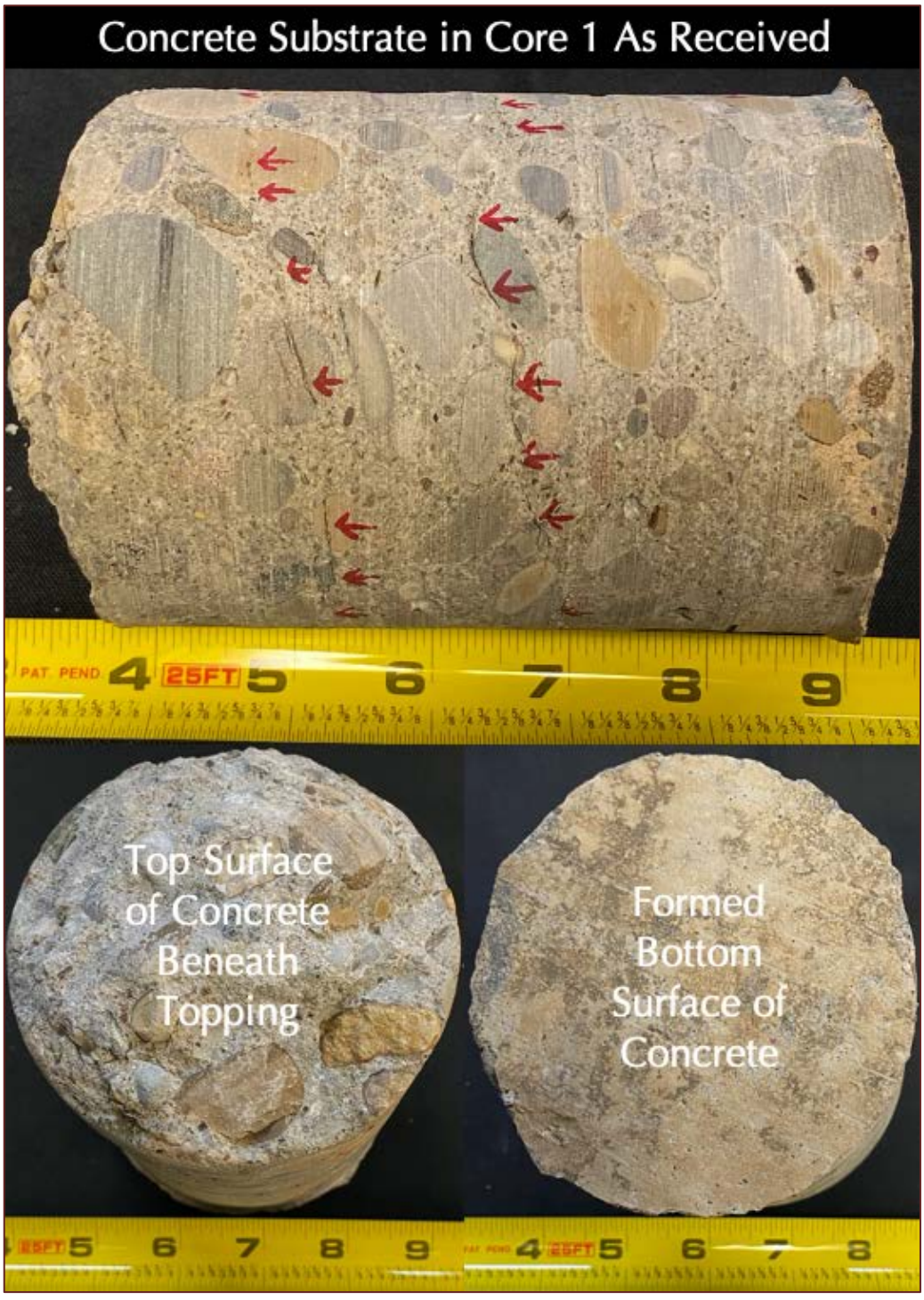

Figure 10: Continuation of overall condition of concrete substrate as seen in Core 1.

Through-depth cracks are marked that have transected and circumscribed the aggregate particles.

Concrete shows the presence of gravel coarse aggregate particles that are well-graded and well-distributed.

Figure 11: Core 2 as received showing:

(a) A 2-in. thick topping entirely detached from a severely rubbled concrete substrate;

(b) Dense, sound, and well-consolidated nature of topping,

(c) Extensive cracking and fragmentation of the concrete substrate to turn into a bag full of rubbles;

(d) Exposed weathered surface of topping and relatively flat underside of topping showing a more or less clean separation from the concrete substrate with no sign of a good bond between the two components; and,

(e) Fractured top and bottom ends of concrete substrate where the bottom end in the bottom right photo shows beige discoloration of paste due to atmospheric carbonation of the underside of the suspended slab above the underground vault. Also present are reddish-brown corrosion products on this concrete chunk that represent carbonation-induced corrosion of steel situated within this carbonated zone near the underside surface of the suspended slab that has received carbon dioxide from the vault's air.

Figure 12: Core 3 as received showing:

(a) A 2-in. thick topping entirely detached from concrete substrate;

(b) Dense, sound, and well-consolidated nature of topping,

(c) A few rubbles of concrete between topping and fractured top surface of concrete;

(d) Lack of extensive through-depth cracking in the concrete substrate that are oriented parallel to the top surface in Core 1; however, this core also contains similar through-depth cracks but at micro scale that were revealed during subsequent treatment of core with fluorescent dye;

(e) Overall intact condition of concrete despite through-depth cracking;

(f) Exposed weathered surface of topping and relatively flat underside of topping showing a more or less clean separation from the concrete substrate with no sign of a good bond between the two components; and

(g) Fractured top and bottom ends of concrete substrate where the bottom end in the bottom right photo shows beige discoloration of paste due to atmospheric carbonation of the underside of the suspended slab above the underground vault. Also present are reddish-brown corrosion products on this concrete chunk that represent carbonation-induced corrosion of steel situated within this carbonated zone near the underside surface of the suspended slab that has received carbon dioxide from the vault's air.

Figure 13: Shown are a few concrete rubbles collected from three cores that show white coating of secondary deposits on the surfaces. These coatings are mostly composed of carbonated products of leached materials from concrete that are removed by migration of moisture through the concrete.

PETROGRAPHIC EXAMINATIONS

LAPPED CROSS SECTIONS

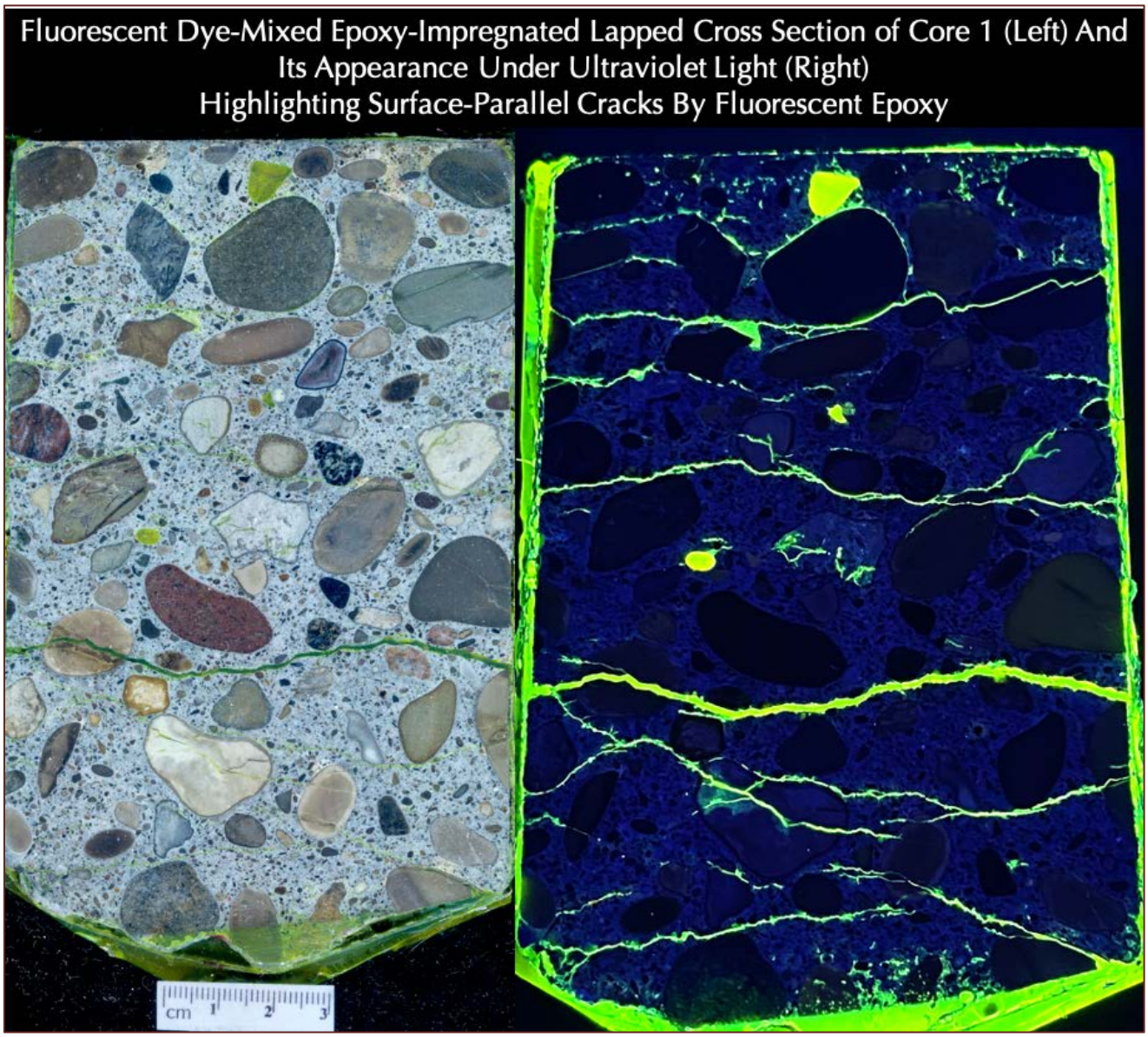

Figure 14: Lapped cross section of Core 1 shown after impregnating with a low-viscosity fluorescent dye-mixed epoxy under vacuum. Left photo shows the scanned image of the lapped cross section where a few visible cracks are seen but the right photo shows the same lapped cross section in a dark room after exposing it to an ultraviolet light where extensive through-depth cracks are revealed by the fluorescent epoxy.

Lapped cross section shows the presence of: (a) gravel coarse aggregate particles having a nominal maximum size of 1 in. (25 mm) where particles are variably dense, many with weathering and/or reaction rims, well-graded, well-distributed, variably colored from light to medium gray, brown, red, black, etc., (b) natural sand fine aggregate having a nominal maximum size of $^{3}/_{8}$ in. (9.5 mm) where particles are variably dense, well-graded, well-distributed, variably colored, and (c) interstitial Portland cement paste of more or less uniform appearance and color tone throughout the depth.

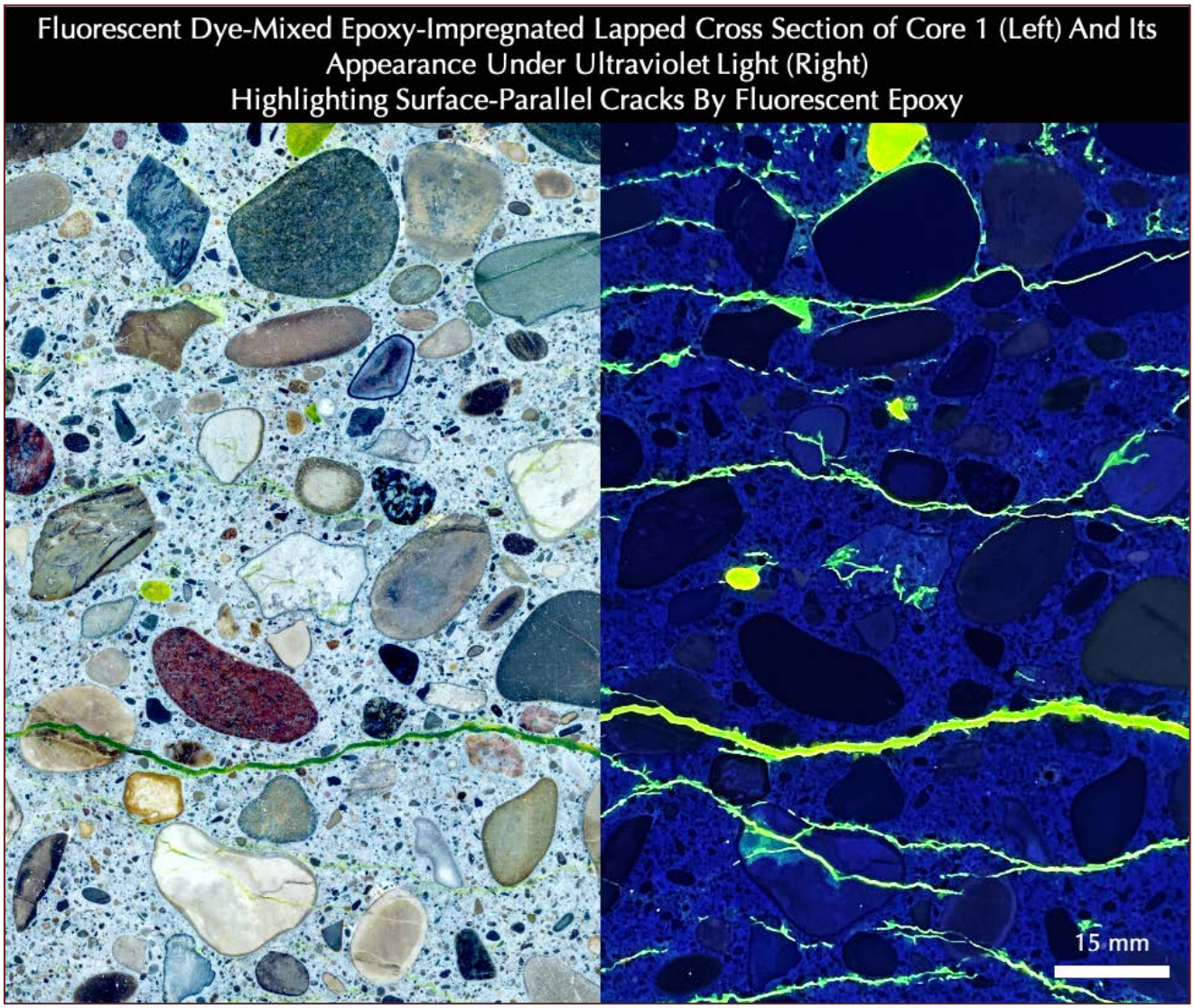

Figure 15: Lapped cross section of Core 1 shown after impregnating with a low-viscosity fluorescent dye-mixed epoxy under vacuum. Left photo shows the scanned image of the lapped cross section where a few visible cracks are seen but the right photo shows the same lapped cross section in a dark room after exposing it to an ultraviolet light where extensive through-depth cracks were revealed by the fluorescent epoxy.

Lapped cross section shows the presence of: (a) gravel coarse aggregate particles having a nominal maximum size of 1 in. (25 mm) where particles are variably dense, many with weathering and/or reaction rims, well-graded, well-distributed, variably colored from light to medium gray, brown, red, black, etc., (b) natural sand fine aggregate having a nominal maximum size of $^{3}/_{8}$ in. (9.5 mm) where particles are variably dense, well-graded, well-distributed, variably colored, and (c) interstitial Portland cement paste of more or less uniform appearance and color tone throughout the depth.

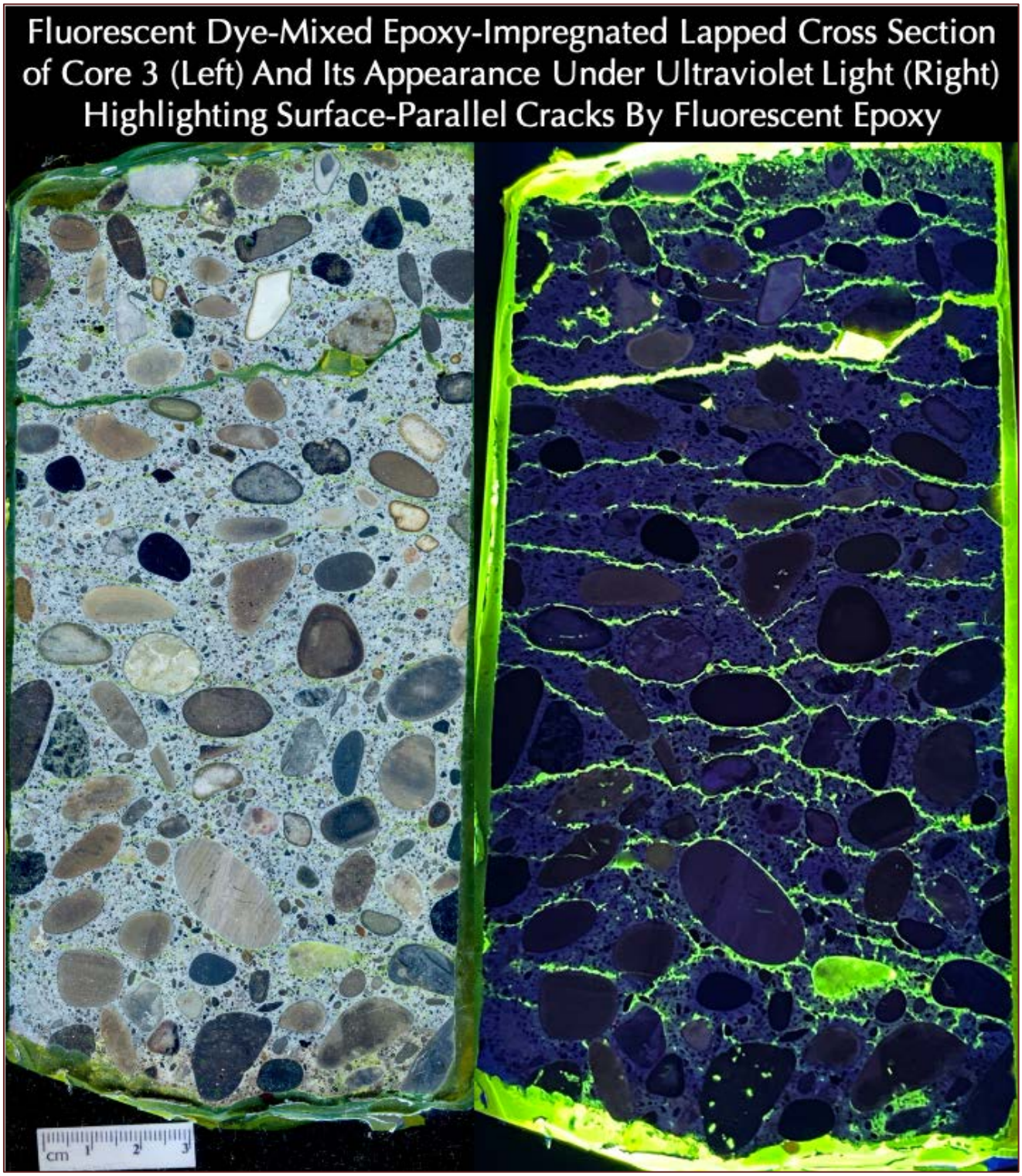

Figure 16: Lapped cross section of Core 3 shown after impregnating with a low-viscosity fluorescent dye-mixed epoxy under vacuum. Left photo shows the scanned image of the lapped cross section where a few visible cracks are seen, but the right photo shows the same lapped cross section in a dark room after exposing it to an ultraviolet light where extensive through-depth cracks were revealed by the fluorescent epoxy.

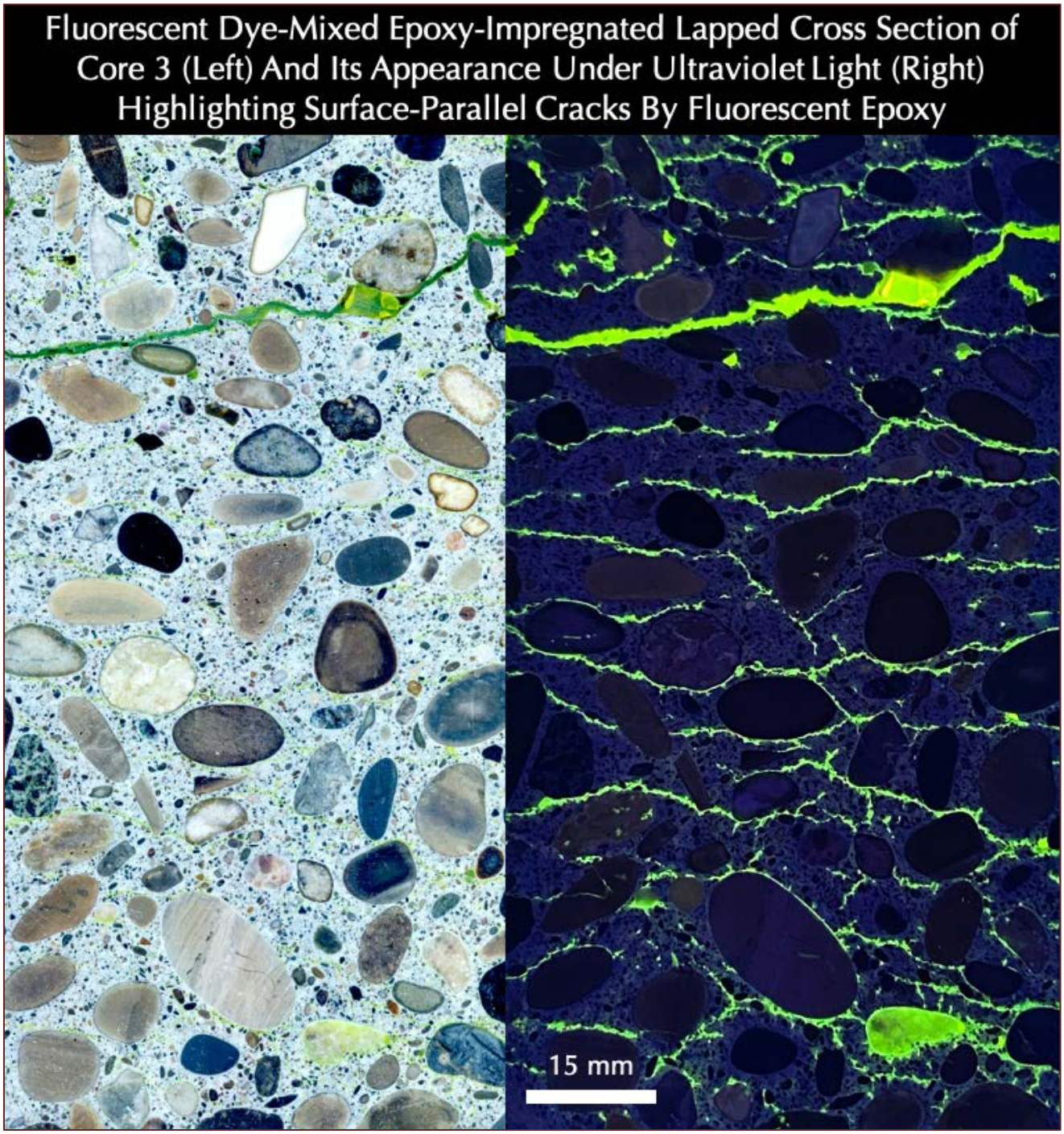

Figure 17: Lapped cross section of Core 3 shown after impregnating with a low-viscosity fluorescent dye-mixed epoxy under vacuum. Left photo shows the scanned image of the lapped cross section where a few visible cracks are seen but the right photo shows the same lapped cross section in a dark room after exposing it to an ultraviolet light where extensive through-depth cracks were revealed by the fluorescent epoxy.

Lapped cross section shows the presence of: (a) gravel coarse aggregate particles having a nominal maximum size of 1 in. (25 mm) where particles are variably dense, many with weathering and/or reaction rims, well-graded, well-distributed, variably colored from light to medium gray, brown, red, black, etc., (b) natural sand fine aggregate having a nominal maximum size of $^{3}/_{8}$ in. (9.5 mm) where particles are variably dense, well-graded, well-distributed, variably colored, and (c) interstitial Portland cement paste of more or less uniform appearance and color tone throughout the depth.

MICROGRAPHS OF LAPPED CROSS SECTIONS

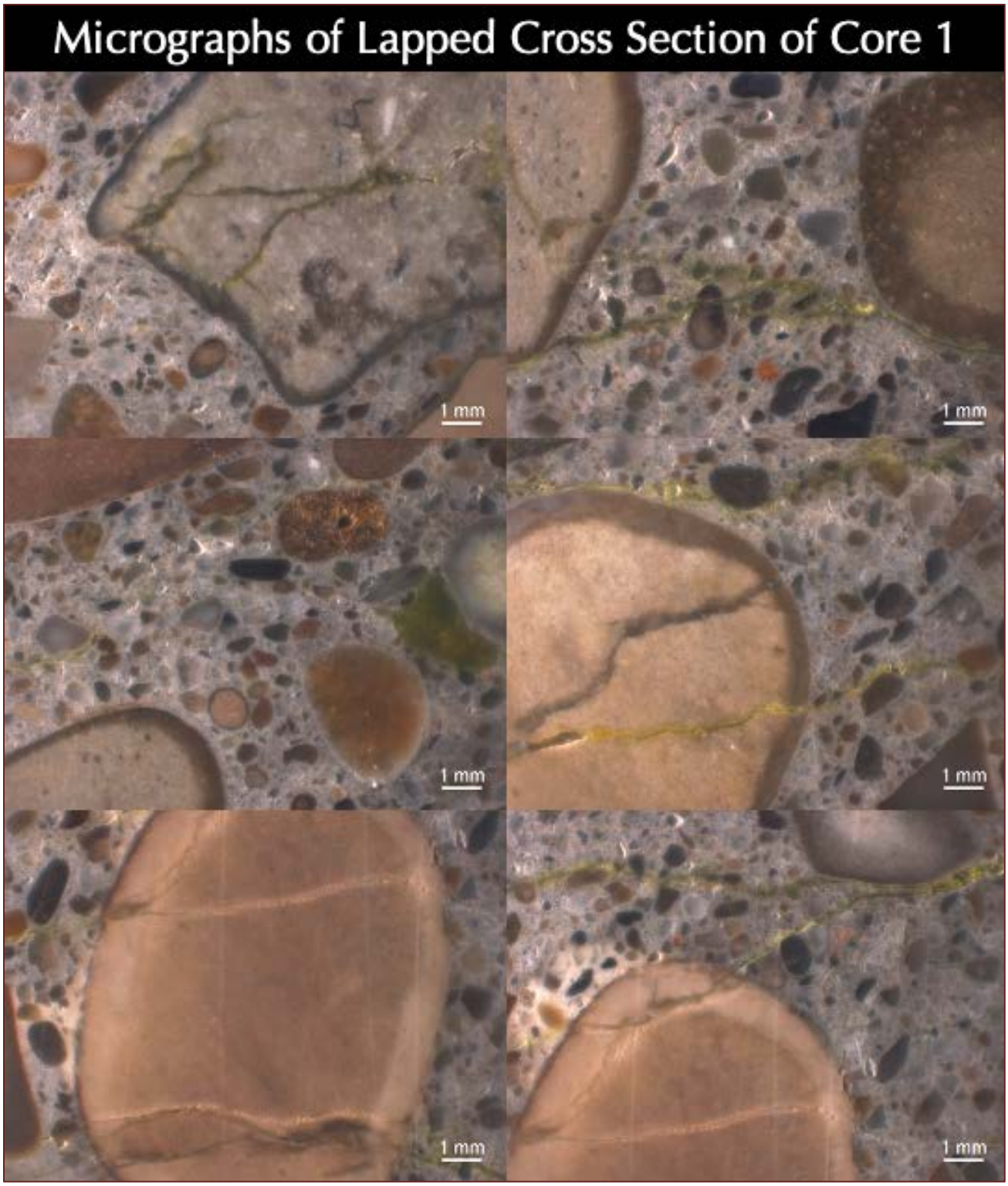

Figure 18: Micrographs of lapped cross section of Core 1 showing: (a) extensive cracking in the concrete where cracks have transected and/or circumscribed the aggregate particles; (b) rounded gravel coarse aggregate particles many showing weathering and/or reaction rims; (c) natural sand fine aggregate; and (d) non-air-entrained nature of concrete. Scale bars are 1 mm.

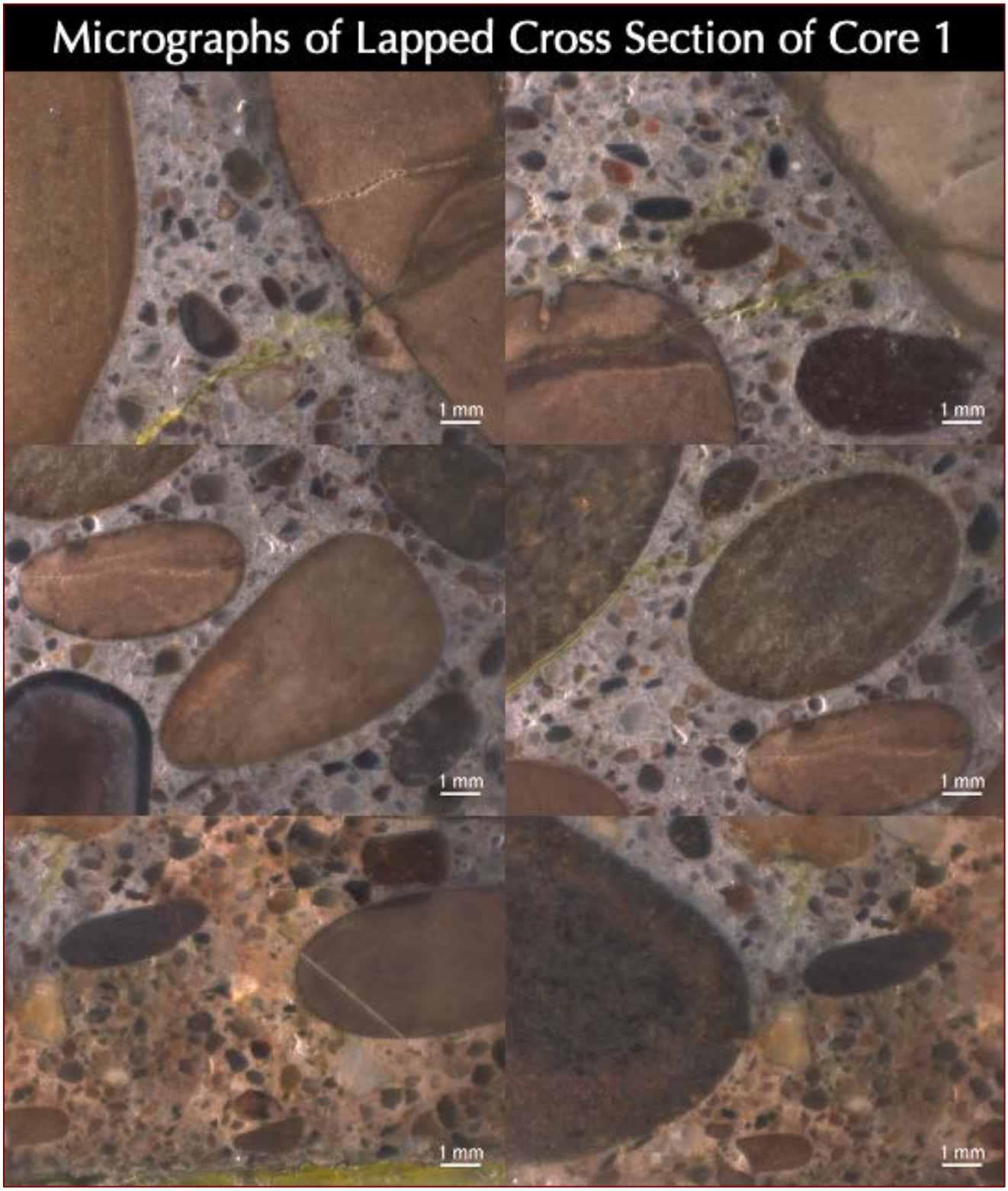

Figure 19: Micrographs of lapped cross section of Core 1 showing: (a) extensive cracking in the concrete where cracks have transected and/or circumscribed the aggregate particles; (b) rounded gravel coarse aggregate particles many showing weathering and/or reaction rims; (c) natural sand fine aggregate; (d) non-air-entrained nature of concrete; and (e) beige discoloration of concrete at the bottom end of core (seen in the bottom row photos) due to atmospheric carbonation from the air inside the vault that has interacted with the underside of the top suspended slab. Scale bars are 1 mm.

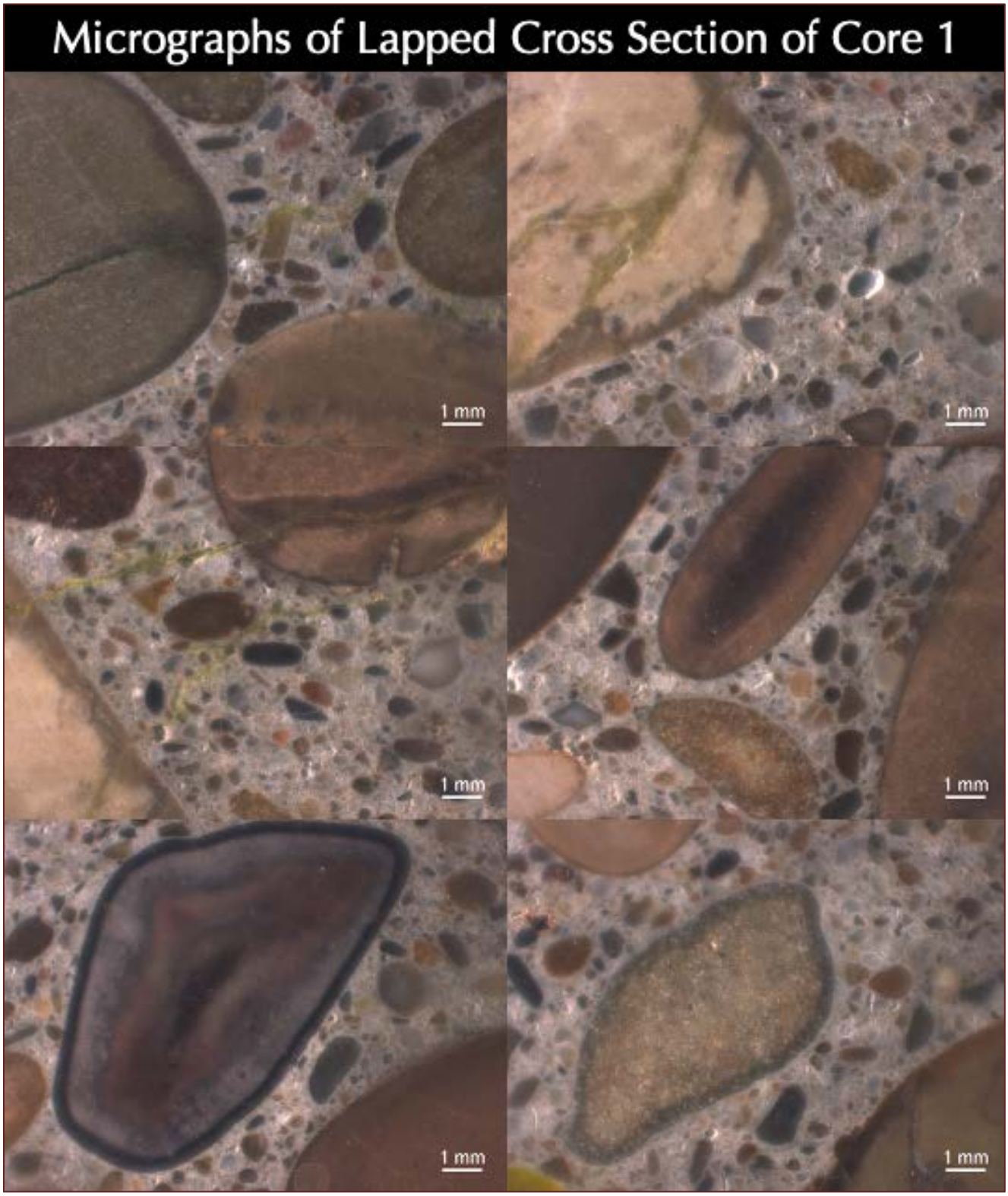

Figure 20: Micrographs of lapped cross section of Core 1 showing: (a) extensive cracking in the concrete where cracks have transected and/or circumscribed the aggregate particles; (b) rounded gravel coarse aggregate particles many showing weathering and/or reaction rims; (c) natural sand fine aggregate; and (d) non-air-entrained nature of concrete. Scale bars are 1 mm.

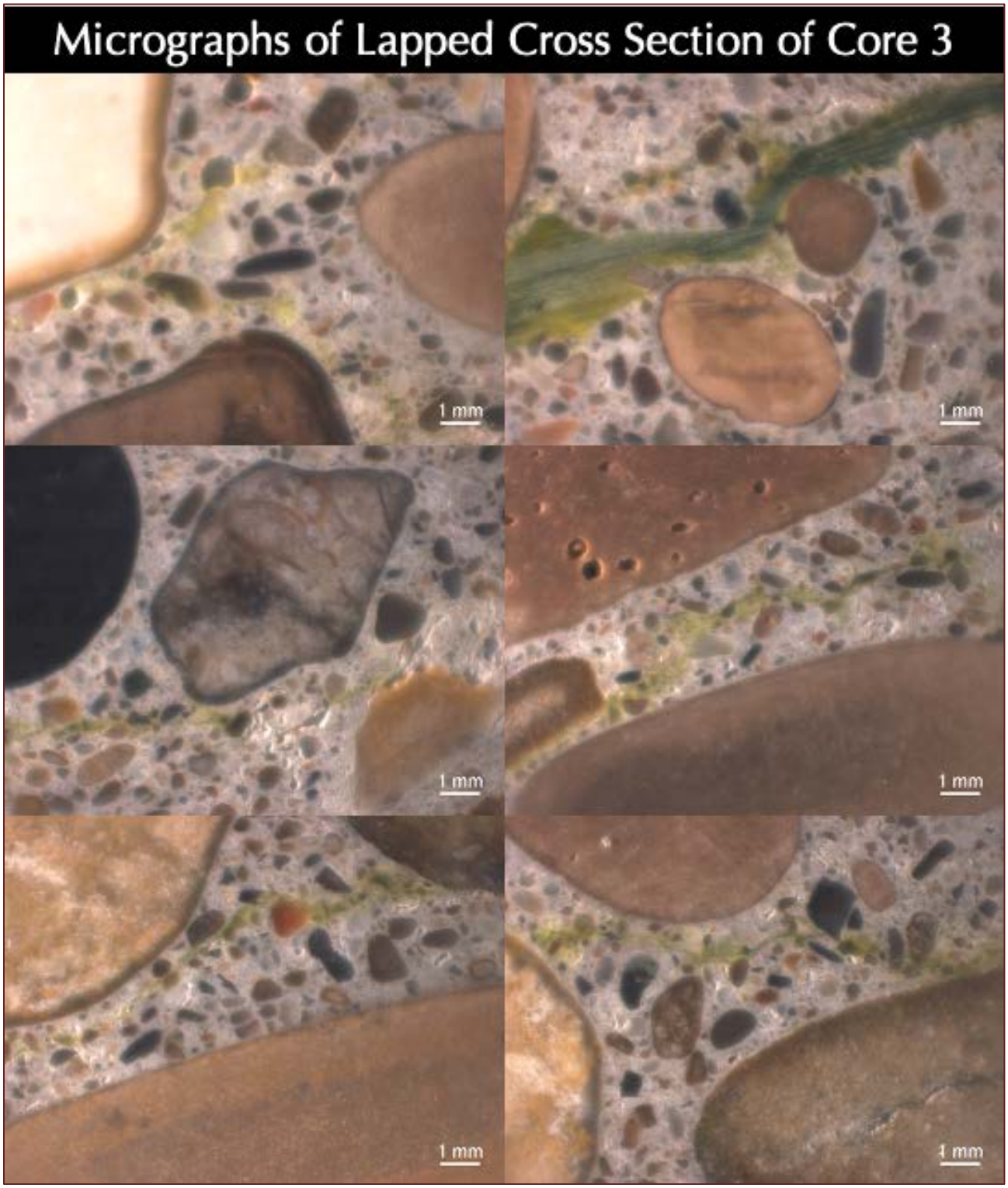

Figure 21: Micrographs of lapped cross section of Core 3 showing: (a) extensive cracking in the concrete where cracks have transected and/or circumscribed the aggregate particles; (b) rounded gravel coarse aggregate particles many showing weathering and/or reaction rims; (c) natural sand fine aggregate; and (d) non-air-entrained nature of concrete. Scale bars are 1 mm.

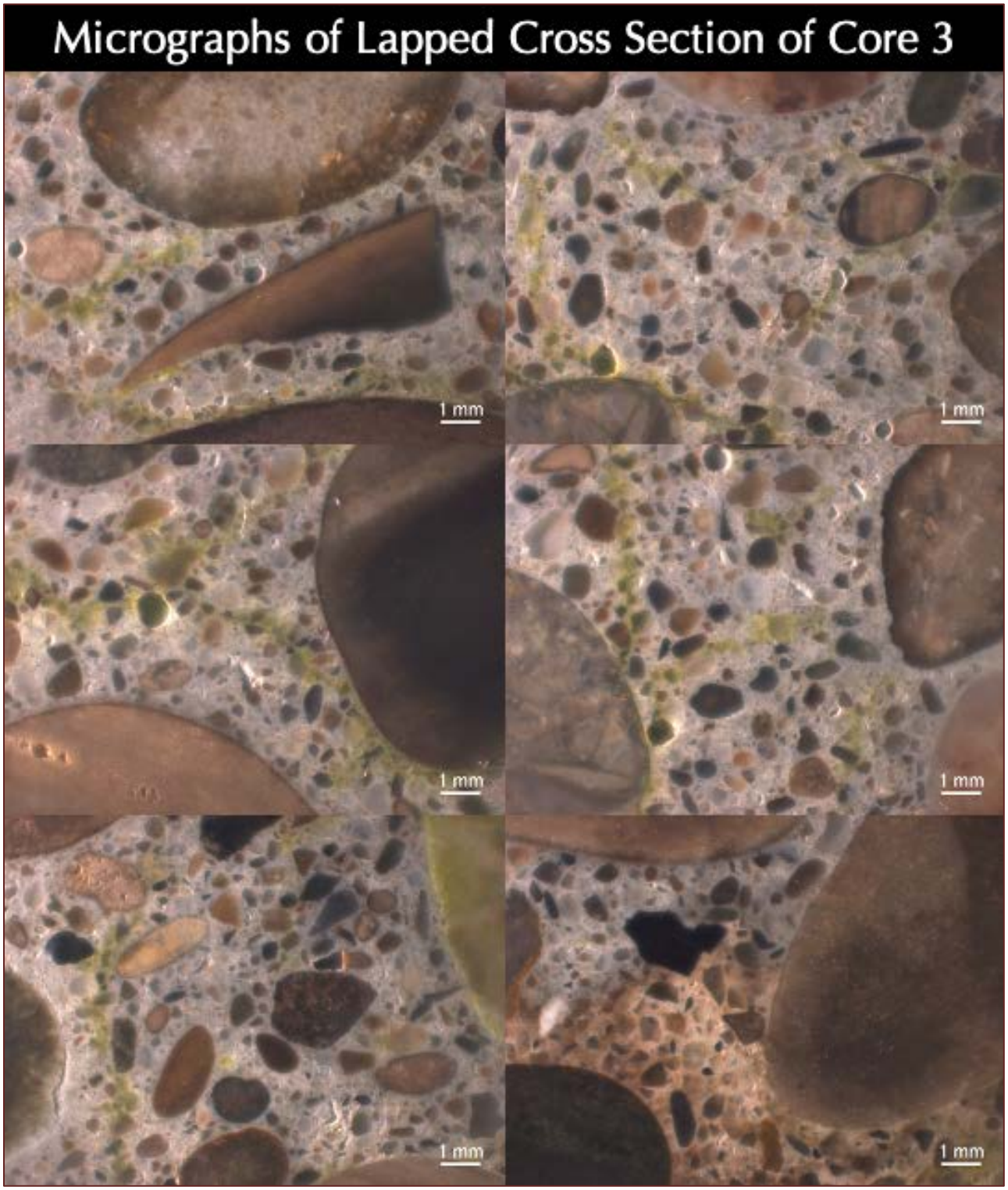

Figure 22: Micrographs of lapped cross section of Core 3 showing: (a) extensive cracking in the concrete where cracks have transected and/or circumscribed the aggregate particles; (b) rounded gravel coarse aggregate particles many showing weathering and/or reaction rims; (c) natural sand fine aggregate; (d) non-air-entrained nature of concrete; and (e) beige discoloration of concrete at the bottom end of core (seen in the bottom right photo) due to atmospheric carbonation from the air inside the vault that has interacted with the underside of the top suspended slab. Scale bars are 1 mm.

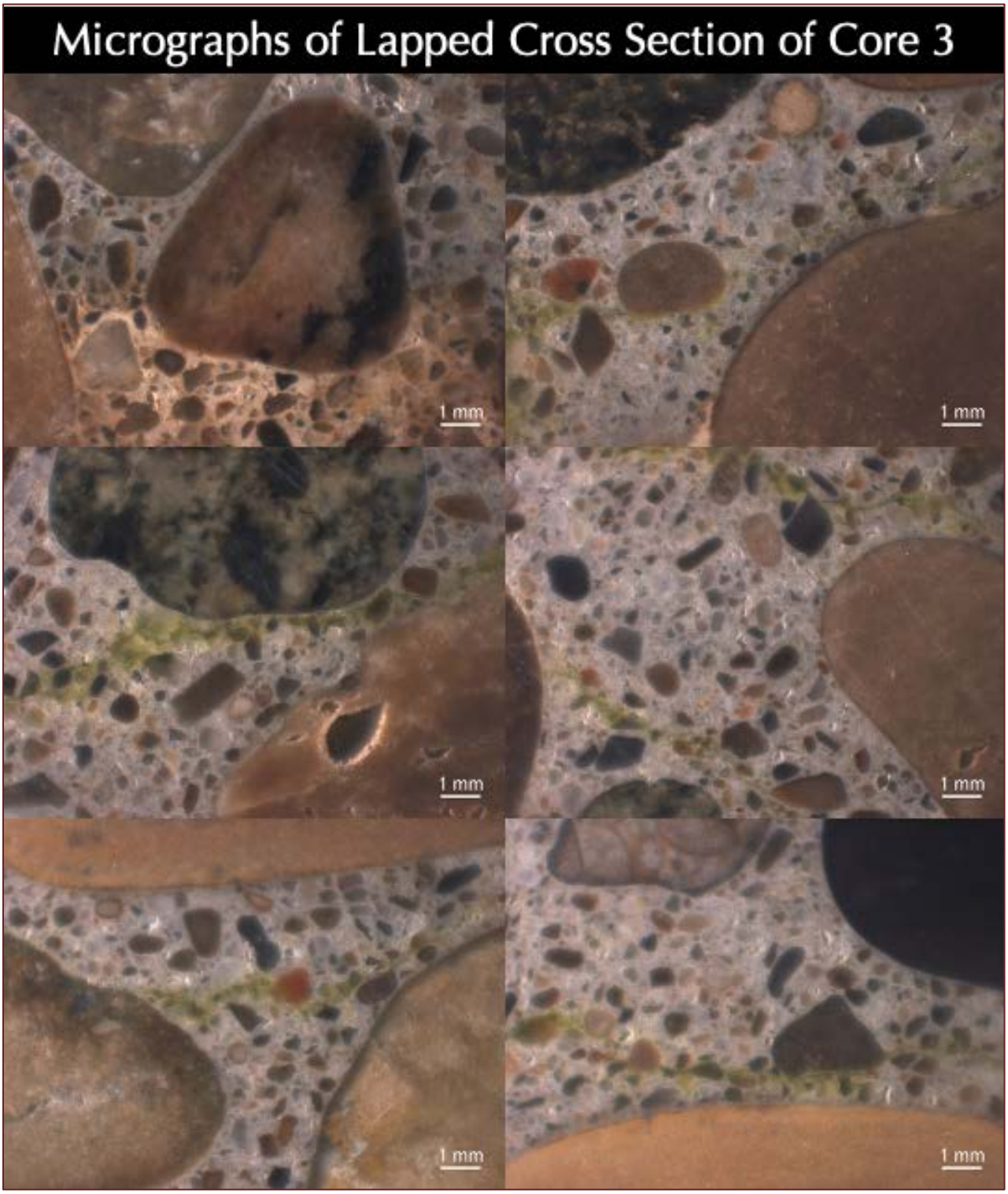

Figure 23: Micrographs of lapped cross section of Core 3 showing: (a) extensive cracking in the concrete where cracks have transected and/or circumscribed the aggregate particles; (b) rounded gravel coarse aggregate particles many showing weathering and/or reaction rims; (c) natural sand fine aggregate; (d) non-air-entrained nature of concrete; and (e) beige discoloration of concrete at the bottom end of core (seen in the top left photo) due to atmospheric carbonation from the air inside the vault that has interacted with the underside of the top suspended slab. Scale bars are 1 mm.

THIN SECTIONS

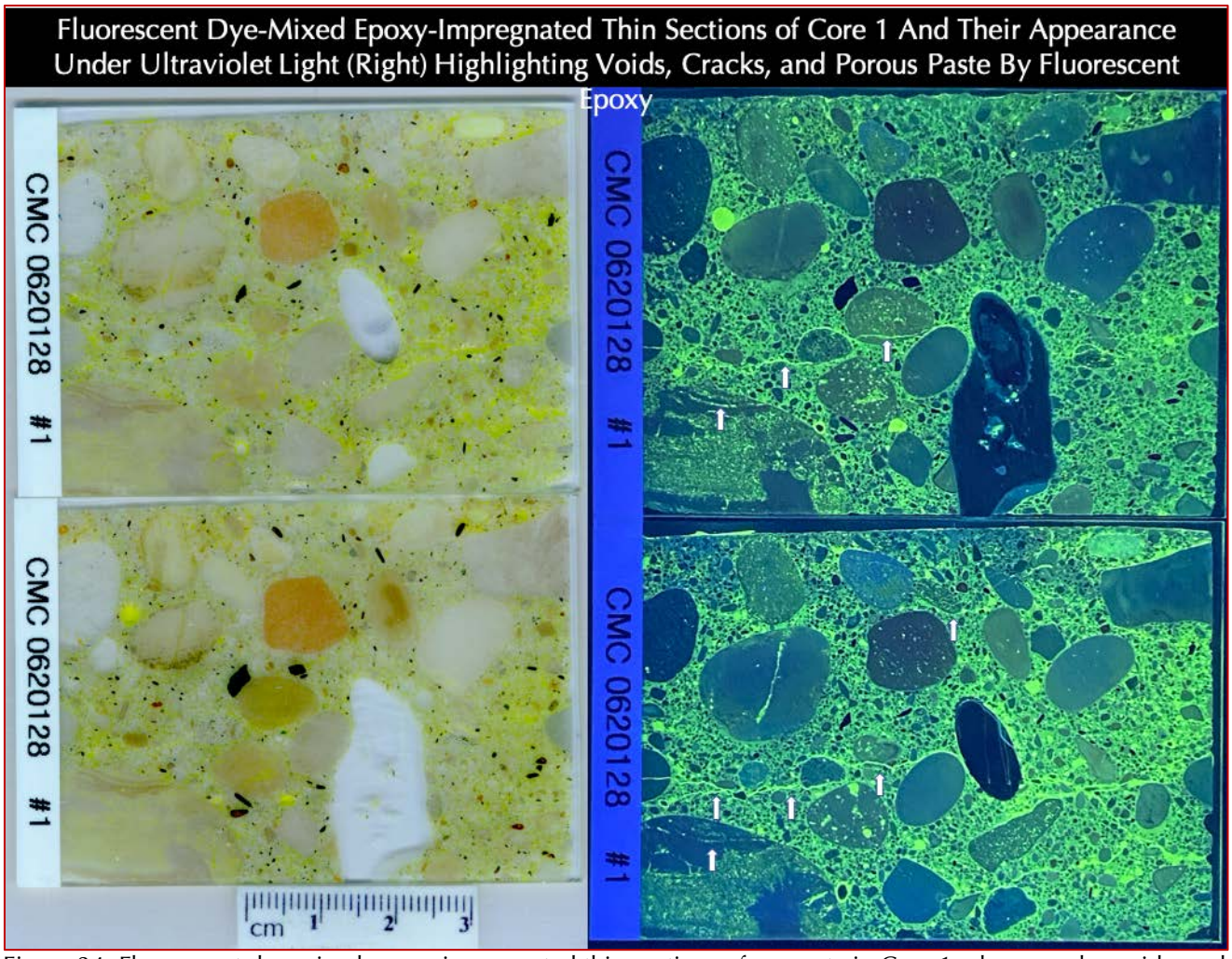

Figure 24: Fluorescent dye-mixed epoxy-impregnated thin sections of concrete in Core 1 where cracks, voids, and porous areas of paste are highlighted by fluorescent epoxy. Thin section shows: (a) rounded gravel coarse aggregate particles; (b) fine sand; and (c) extensive cracks through the depth of section where cracks have transected many aggregate particles. Thin section is approximately 30 microns (0.03 mm) in thickness and transparent to polarized-light.

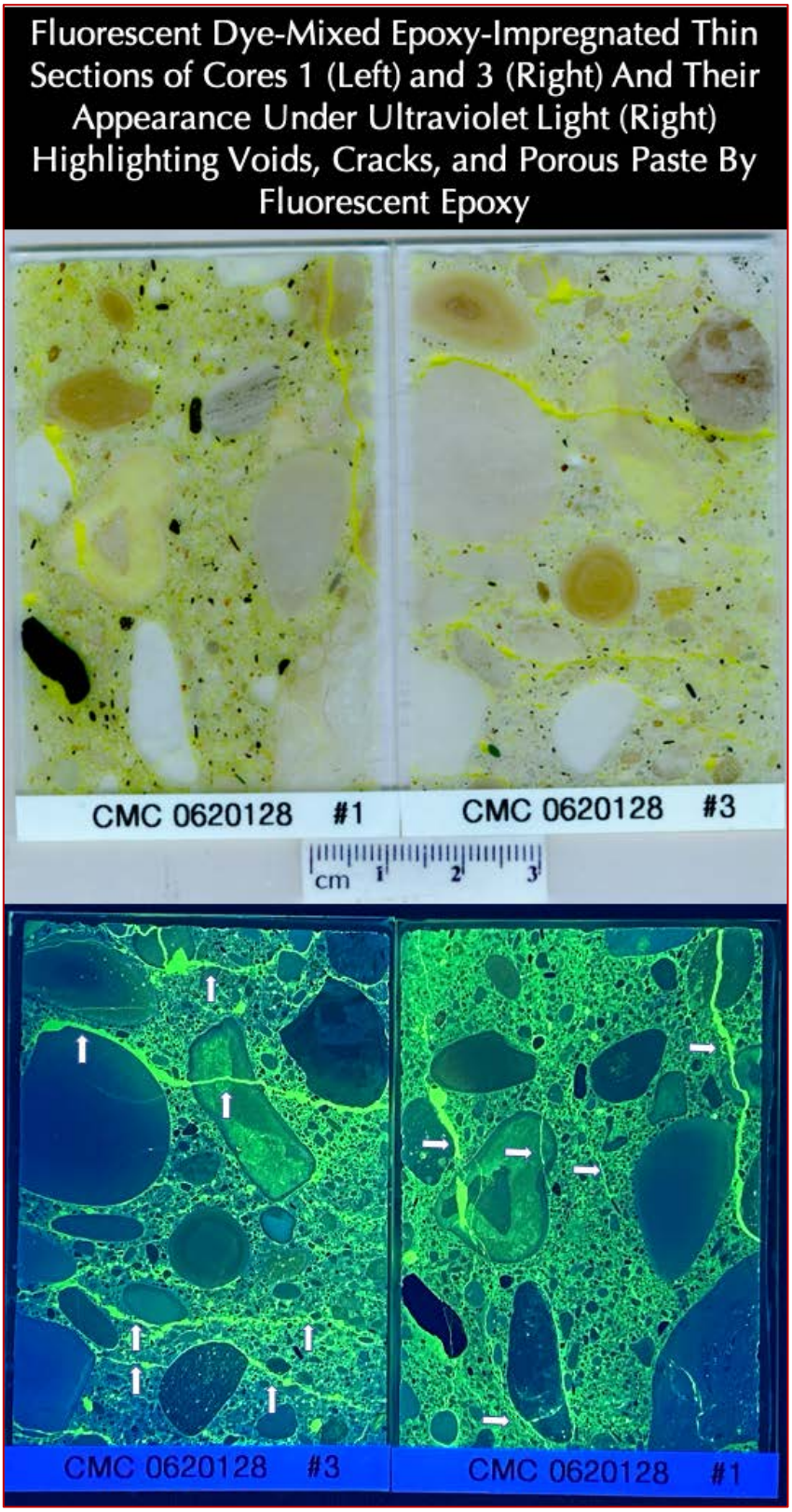

Figure 25: Fluorescent dye-mixed epoxy-impregnated thin sections of concrete in Cores 1 and 3 where cracks, voids, and porous areas of paste are highlighted by fluorescent epoxy. Thin section shows: (a) rounded gravel coarse aggregate particles; (b) fine sand; and (c) extensive cracks through the depth of section where cracks have transected many aggregate particles. Thin section is approximately 30 microns (0.03 mm) in thickness and transparent to polarized-light.

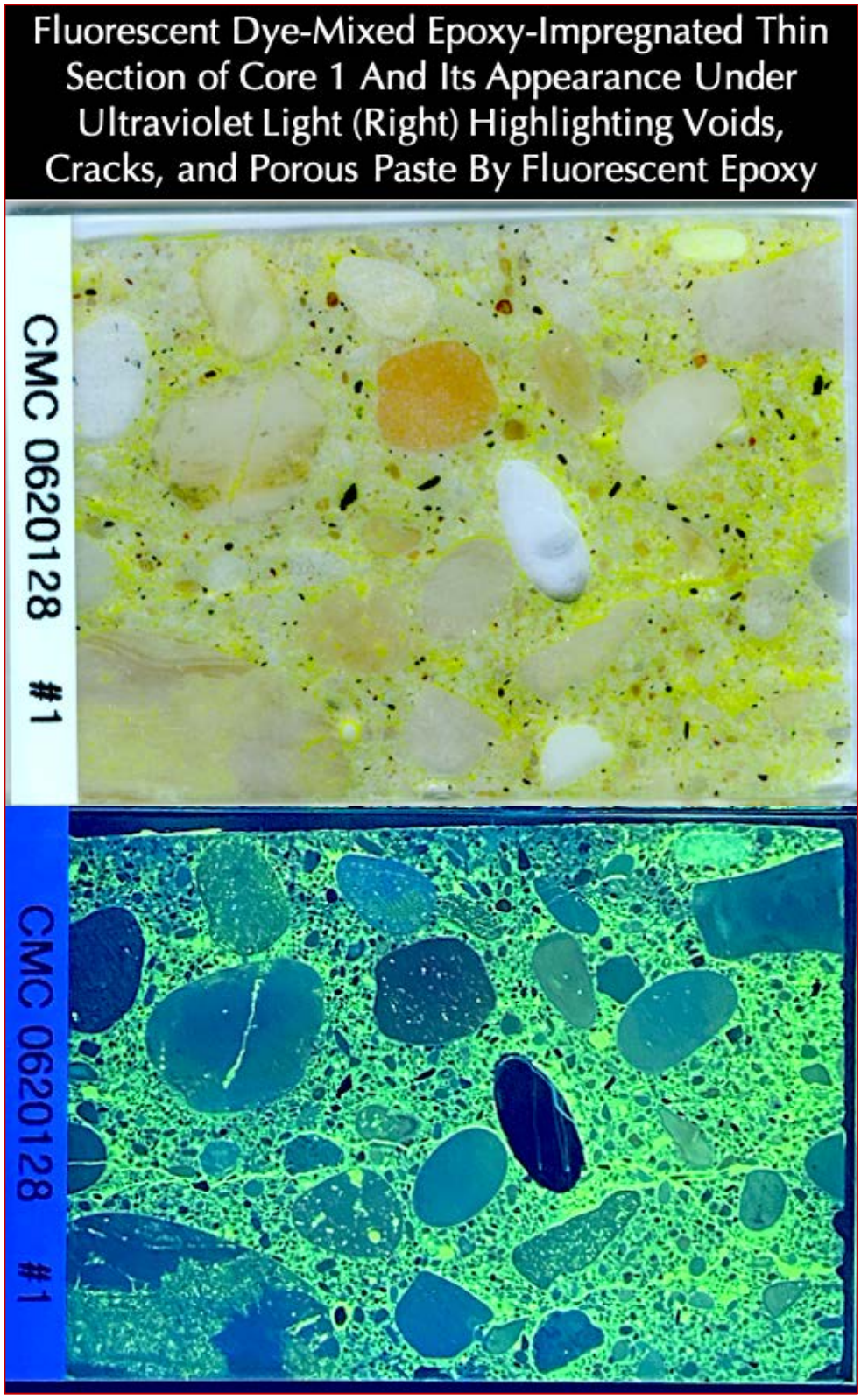

Figure 26: Fluorescent dye-mixed epoxy-impregnated thin section of concrete in Core 1 where cracks, voids, and porous areas of paste are highlighted by fluorescent epoxy. Thin section shows: (a) rounded gravel coarse aggregate particles; (b) fine sand; and (c) extensive cracks through the depth of section where cracks have transected many aggregate particles. Thin section is approximately 30 microns (0.03 mm) in thickness and transparent to polarized-light.

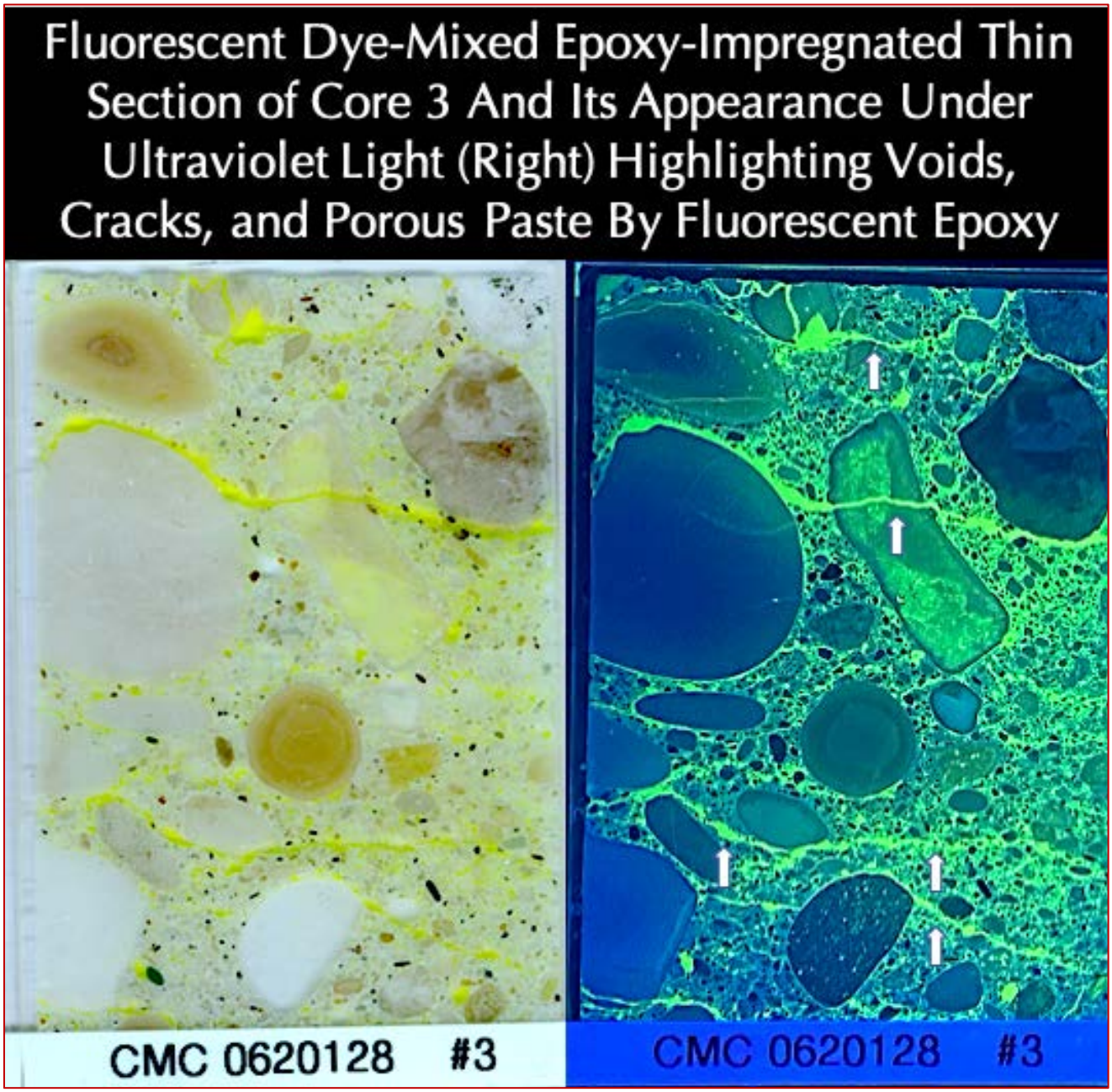

Figure 27: Fluorescent dye-mixed epoxy-impregnated thin section of concrete in Core 3 where cracks, voids, and porous areas of paste are highlighted by fluorescent epoxy. Thin section shows: (a) rounded gravel coarse aggregate particles; (b) fine sand; and (c) extensive cracks through the depth of section where cracks have transected many aggregate particles. Thin section is approximately 30 microns (0.03 mm) in thickness and transparent to polarized-light.

MICROGRAPHS OF THIN SECTIONS

Figure 28: Fluorescent dye-mixed epoxy-impregnated thin section of concrete in Core 1 showing aggregates, paste, air, cracks, and various microstructural features.

Micrographs were taken with a transmitted-light Olympus SZX 12 stereozoom microscope that has transmitted, reflected, polarized, and fluorescent light facilities.

Images were taken at 10X magnification in plane polarized-light mode where field width of each image is 15 mm.

The mosaic of six images represent 30 × 45 mm area of thin section where cracks, gravel coarse aggregate particles and interstitial mortar fraction of sand and Portland cement paste are seen.

Figure 29: Fluorescent dye-mixed epoxy-impregnated thin section of concrete in Core 1 showing aggregates, paste, air, cracks, and various microstructural features.

Micrographs were taken with a transmitted-light Olympus SZX 12 stereozoom microscope that has transmitted, reflected, polarized, and fluorescent light facilities.

Images were taken at 10X magnification in crossed polarized-light mode, where field width of each image is 15 mm.

The mosaic of six images represent 30 × 45 mm area of thin section where cracks, calcareous gravel coarse aggregate particles and interstitial mortar fraction of siliceous-calcareous sand and variably carbonated Portland cement paste are seen.

Figure 30: Fluorescent dye-mixed epoxy-impregnated thin section of concrete in Core 1 showing aggregates, paste, air, cracks, and various microstructural features.

Micrographs were taken with a transmitted-light Olympus SZX 12 stereozoom microscope that has transmitted, reflected, polarized, and fluorescent light facilities.

Images were taken at 10X magnification in crossed polarized-light mode, where field width of each image is 15 mm.

The mosaic of six images represent 30 × 45 mm area of thin section where cracks, calcareous gravel coarse aggregate particles and interstitial mortar fraction of siliceous-calcareous sand and variably carbonated Portland cement paste are seen.

Figure 31: Fluorescent dye-mixed epoxy-impregnated thin section of concrete in Core 3 showing aggregates, paste, air, cracks, and various microstructural features.

Micrographs were taken with a transmitted-light Olympus SZX 12 stereozoom microscope that has transmitted, reflected, polarized, and fluorescent light facilities.

Images were taken at 10X magnification in plane polarized-light mode where field width of each image is 15 mm.

The mosaic of six images represent 30 × 45 mm area of thin section where cracks, gravel coarse aggregate particles and interstitial mortar fraction of sand and Portland cement paste are seen.

Figure 32: Fluorescent dye-mixed epoxy-impregnated thin section of concrete in Core 3 showing aggregates, paste, air, cracks, and various microstructural features.

Micrographs were taken with a transmitted-light Olympus SZX 12 stereozoom microscope that has transmitted, reflected, polarized, and fluorescent light facilities.

Images were taken at 10X magnification in crossed polarized-light mode, where field width of each image is 15 mm.

The mosaic of six images represent 30 × 45 mm area of thin section where cracks, calcareous gravel coarse aggregate particles and interstitial mortar fraction of siliceous-calcareous sand and variably carbonated Portland cement paste are seen.

Figure 33: Fluorescent dye-mixed epoxy-impregnated thin section of concrete in Core 3 showing aggregates, paste, air, cracks, and various microstructural features.

Micrographs were taken with a transmitted-light Olympus SZX 12 stereozoom microscope that has transmitted, reflected, polarized, and fluorescent light facilities.

Images were taken at 10X magnification in crossed polarized-light mode, where field width of each image is 15 mm.

The mosaic of six images represent 30 × 45 mm area of thin section where cracks, calcareous gravel coarse aggregate particles and interstitial mortar fraction of siliceous-calcareous sand and variably carbonated Portland cement paste are seen.

Figure 34: Fluorescent dye-mixed epoxy-impregnated thin section of concrete in Core 3 showing aggregates, paste, air, cracks, and various microstructural features.

Micrographs were taken with a transmitted-light Olympus SZX 12 stereozoom microscope that has transmitted, reflected, polarized, and fluorescent light facilities.

Images were taken at 10X magnification in crossed polarized-light mode, where field width of each image is 15 mm.

The mosaic of six images represent 30 × 45 mm area of thin section where cracks, calcareous gravel coarse aggregate particles and interstitial mortar fraction of siliceous-calcareous sand and variably carbonated Portland cement paste are seen.

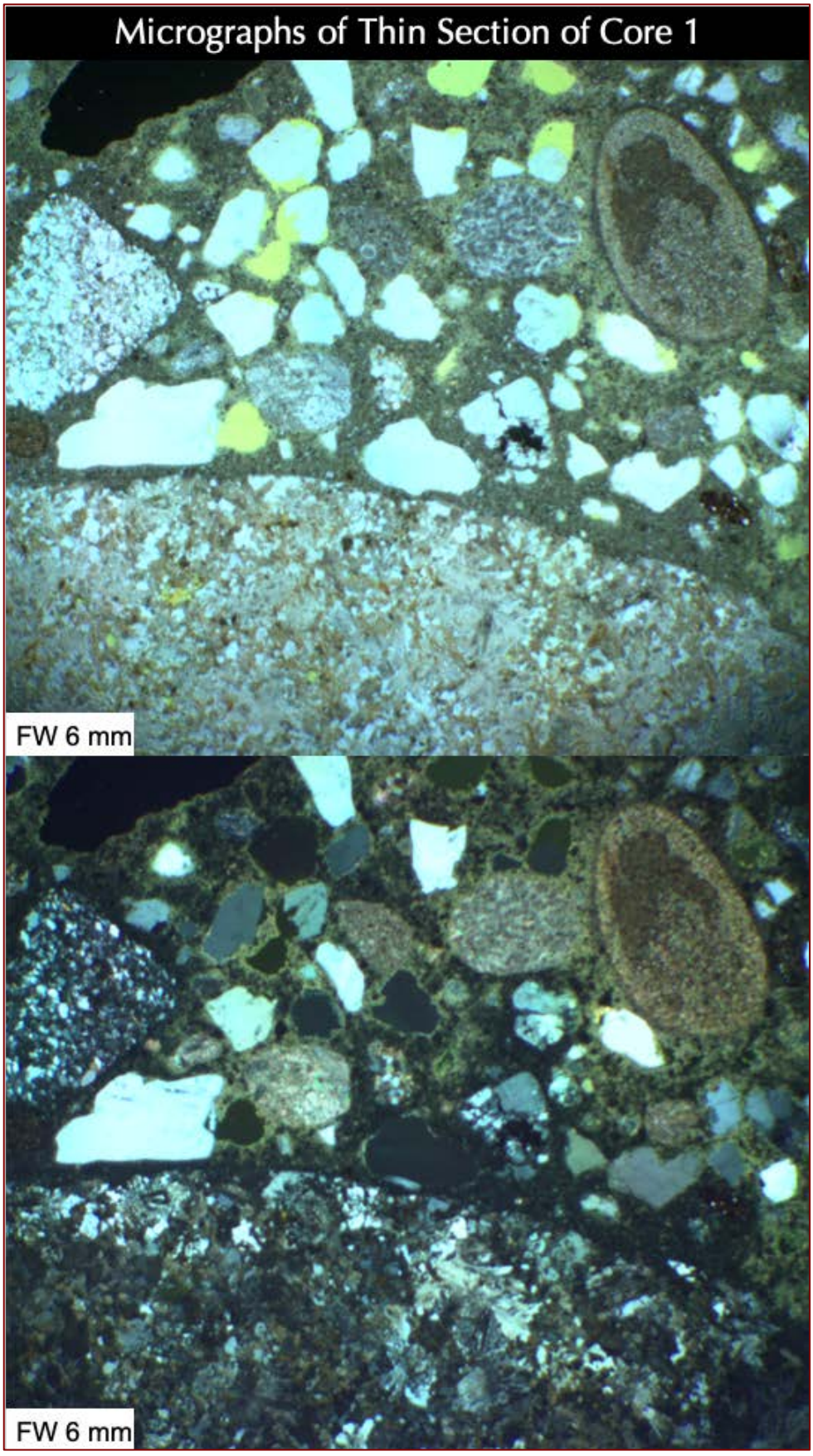

Figure 35: Micrographs of thin section of Core 1 taken in plane (top) and crossed-polarized (bottom) light modes with an Olympus SZX12 stereozoom fluorescent-light microscope with attachments for polarized light showing the non-air-entrained nature of the concrete.

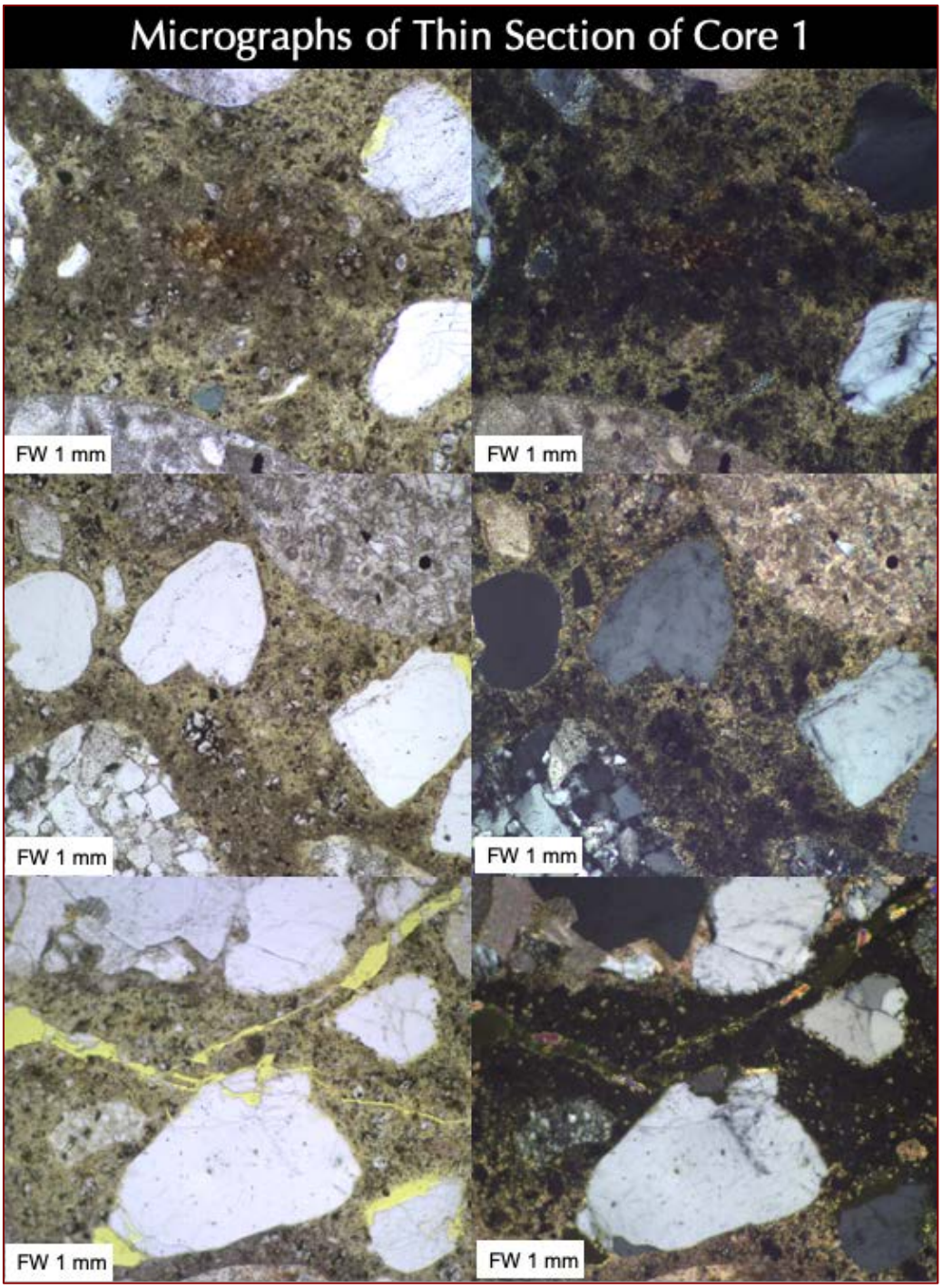

Figure 36: Micrographs of thin section of Core 1 taken in plane and crossed-polarized light modes with a Nikon Eclipse E600 fluorescent-light microscope with an attached Basler camera showing:

(a) Portland cement paste that is variably carbonated, contains many residual cement particles and cement hydration products;

(b) Size, shape, angularity, sphericity, grading, and, distribution of siliceous-calcareous sand fine aggregate particles in concrete; and,

(c) Cracks that are highlighted by fluorescent epoxy.

Photos were taken with a 2X objective to cover the maximum area. Field width of each photo is 1 mm.

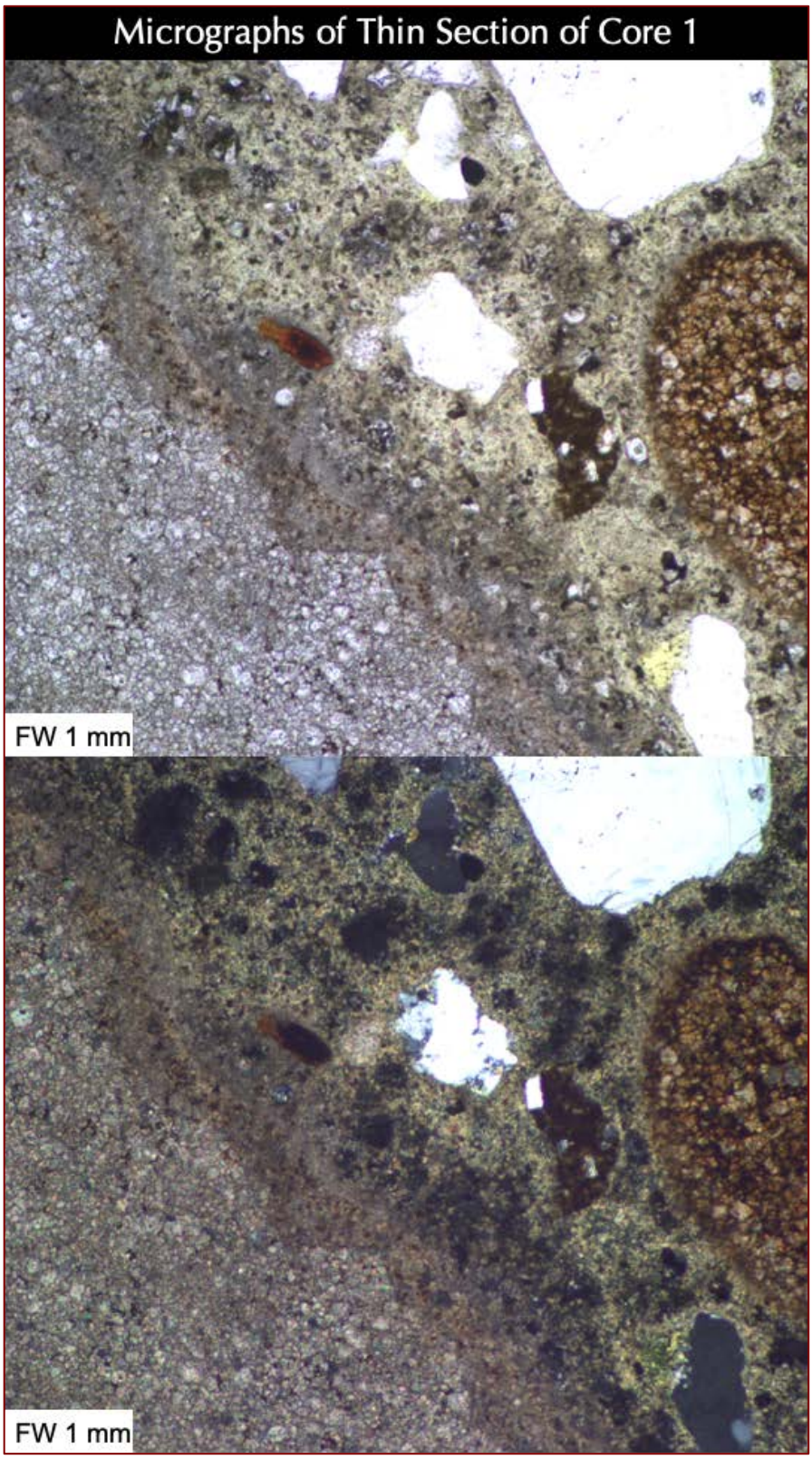

Figure 37: Micrographs of thin section of Core 1 taken in plane and crossed-polarized light modes with a Nikon Eclipse E600 fluorescent-light microscope with an attached Basler camera showing:

(a) Portland cement paste that is variably carbonated, contains many residual cement particles and cement hydration products;

(b) Size, shape, angularity, sphericity, grading, and, distribution of siliceous-calcareous sand fine aggregate particles in concrete; and,

(c) Cracks that are highlighted by fluorescent epoxy.

Photos were taken with a 2X objective to cover the maximum area. Field width of each photo is 1 mm.

Notice a dark low water-cement ratio paste rim along the margin of a porous dolomite gravel particle in coarse aggregate where loss of some water from the paste by absorption of porous limestone gravel coarse aggerate particle has created a dark paste rim.

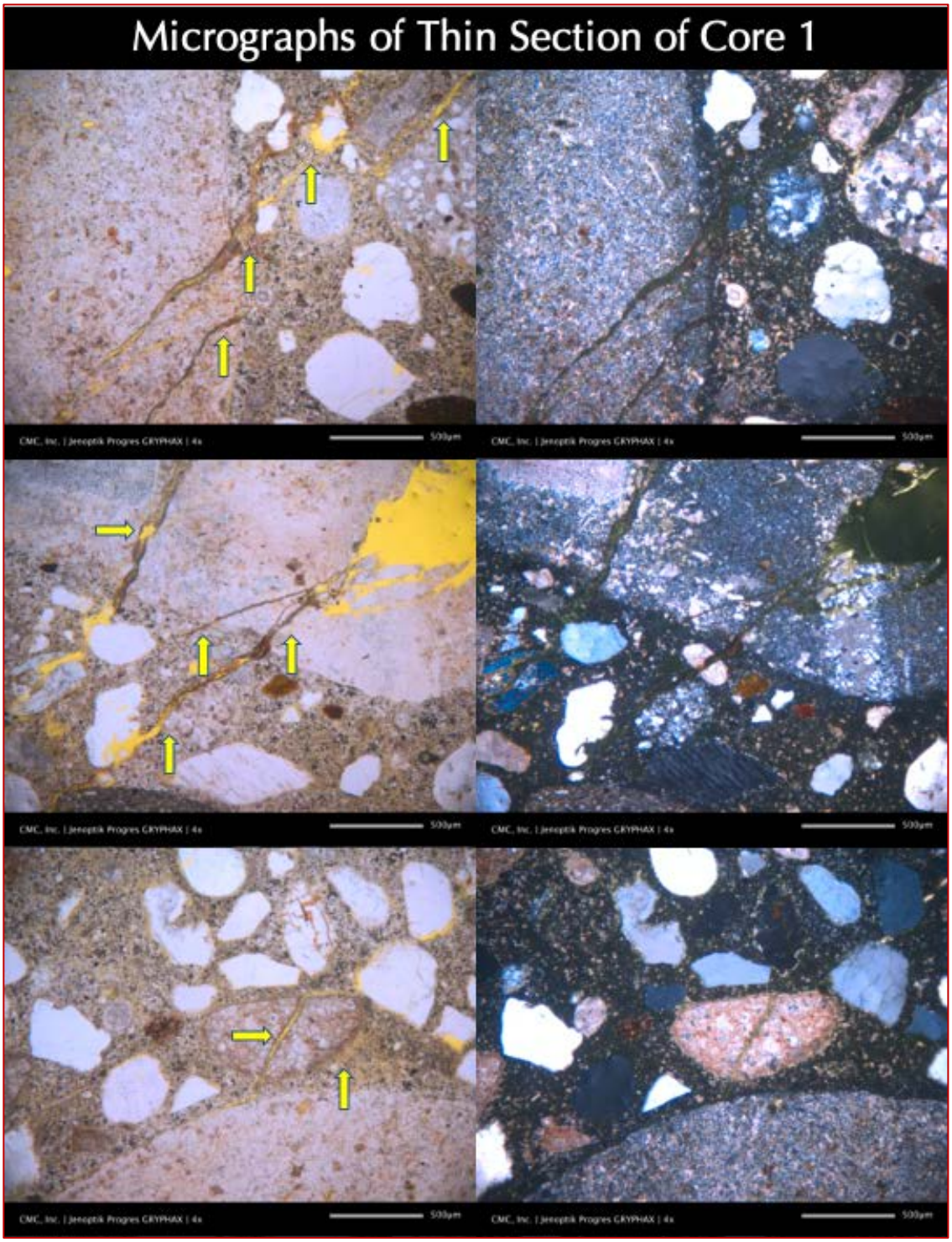

Figure 38: Micrographs of thin section of Core 1 taken with a Nikon Eclipse E600 POL Petrographic microscope with an attached Jenoptik Progres Gryphax camera showing many microcracks extending from cherty limestone and dolomitic chert gravel coarse aggregate particles to the paste where many such cracks from reactive aggregates to paste contain alkali-silica reaction gel formed due to reactions between such potentially reactive fine-grained cryptocrystalline to microcrystalline silica or chert component in limestone or dolomite and high alkali from cement in the presence of moisture. These microcrystalline silica or chert inclusions in limestone and dolomite are found in many gravel coarse aggregate particles across all three cores that are found to be reactive to cement alkalis in the presence of moisture.

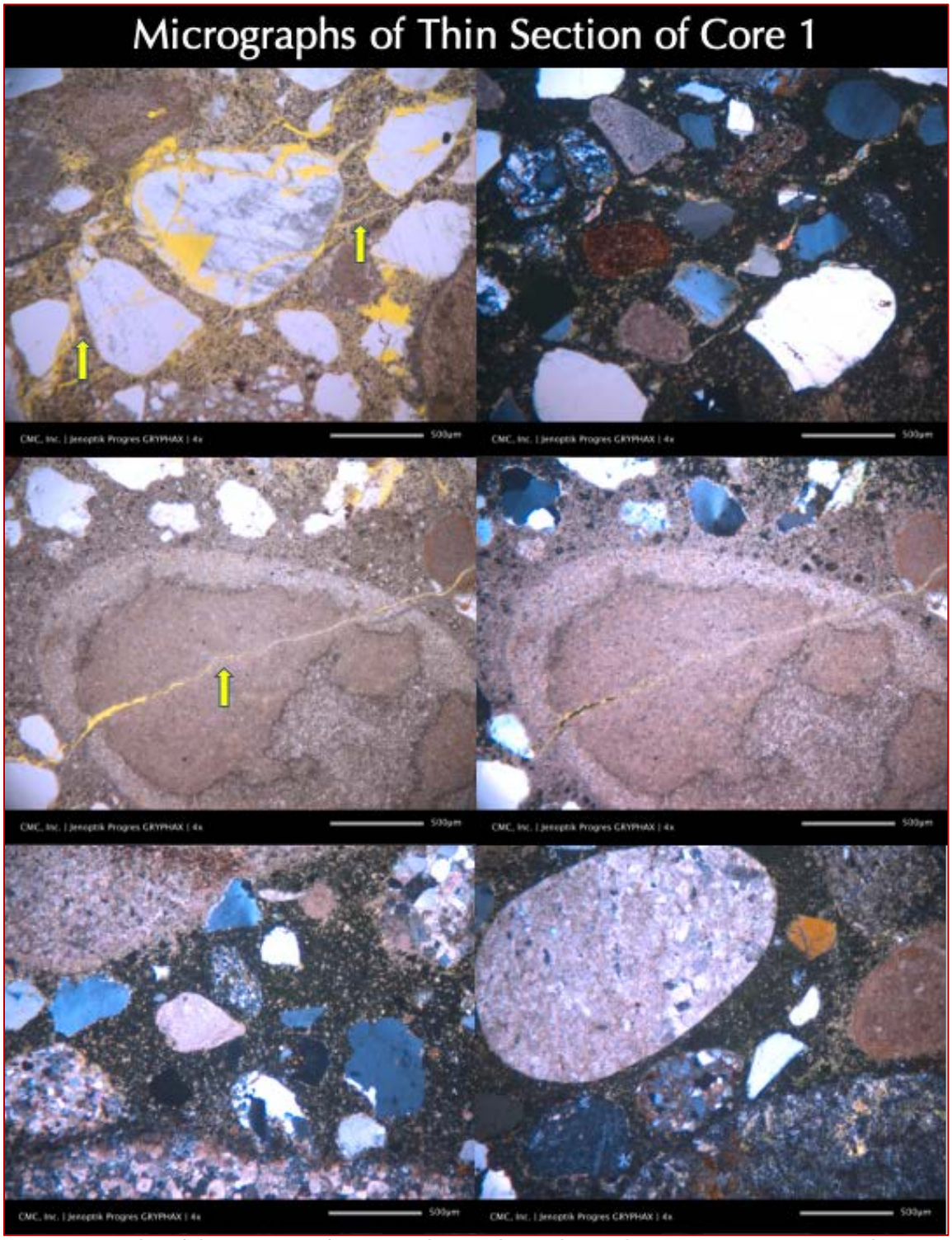

Figure 39: Micrographs of thin section of Core 1 taken with a Nikon Eclipse E600 POL Petrographic microscope with an attached Jenoptik Progres Gryphax camera showing many microcracks extending from cherty limestone and dolomitic chert gravel coarse aggregate particles to the paste where many such cracks from reactive aggregates to paste contain alkali-silica reaction gel formed due to reactions between such potentially reactive fine-grained cryptocrystalline to microcrystalline silica or chert components in limestone or dolomite and high alkali from cement in the presence of moisture. These microcrystalline silica or chert inclusions in limestone and dolomite are found in many gravel coarse aggregate particles across all three cores that are found to be reactive to cement alkalis in the presence of moisture

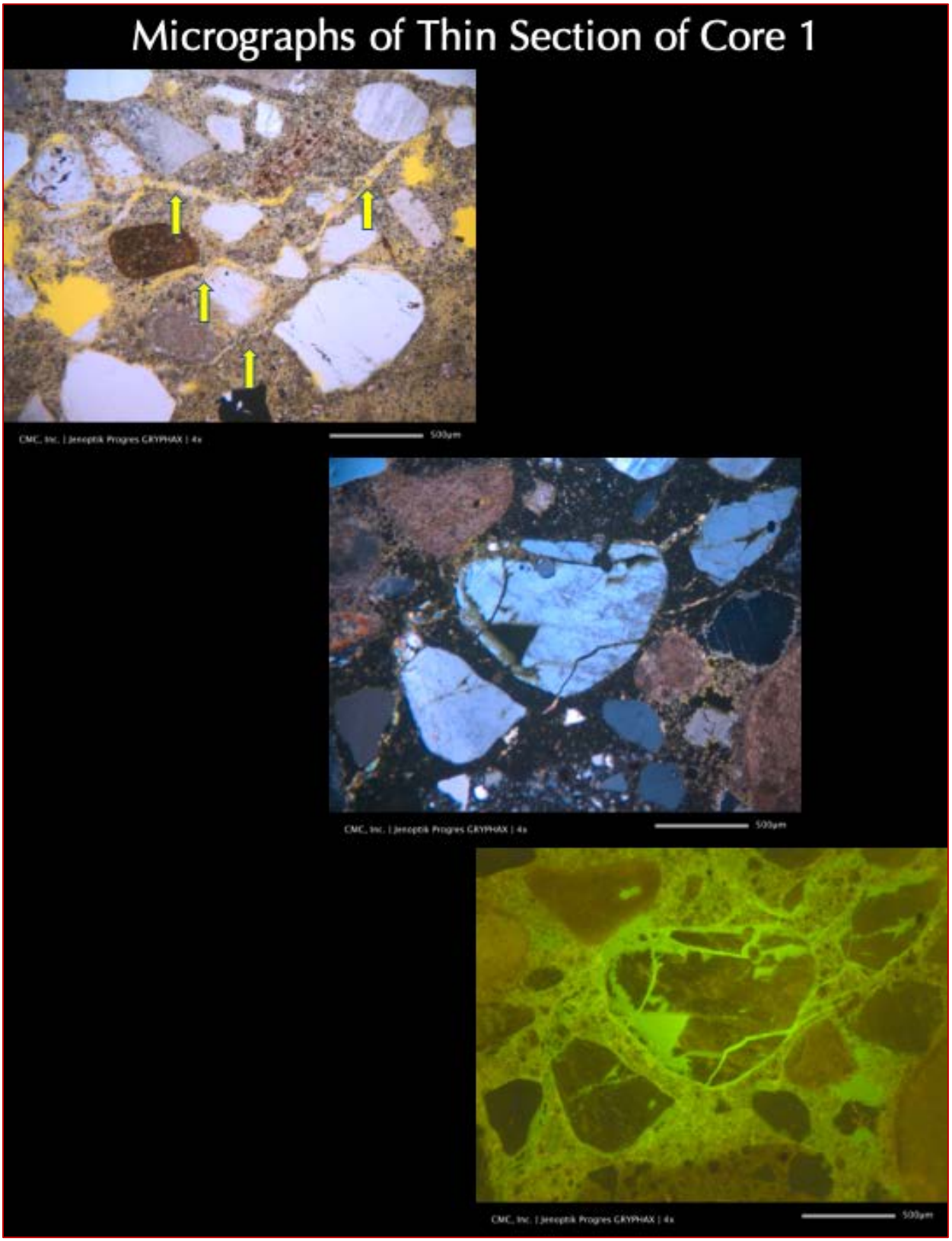

Figure 40: Micrographs of thin section of Core 1 taken with a Nikon Eclipse E600 POL Petrographic microscope with an attached Jenoptik Progres Gryphax camera showing microcracks extending in concrete transected and circumscribed the aggregate particles. Cracks are highlighted by fluorescent epoxy in plane, crossed, and fluorescent light modes from the top to bottom images, respectively.

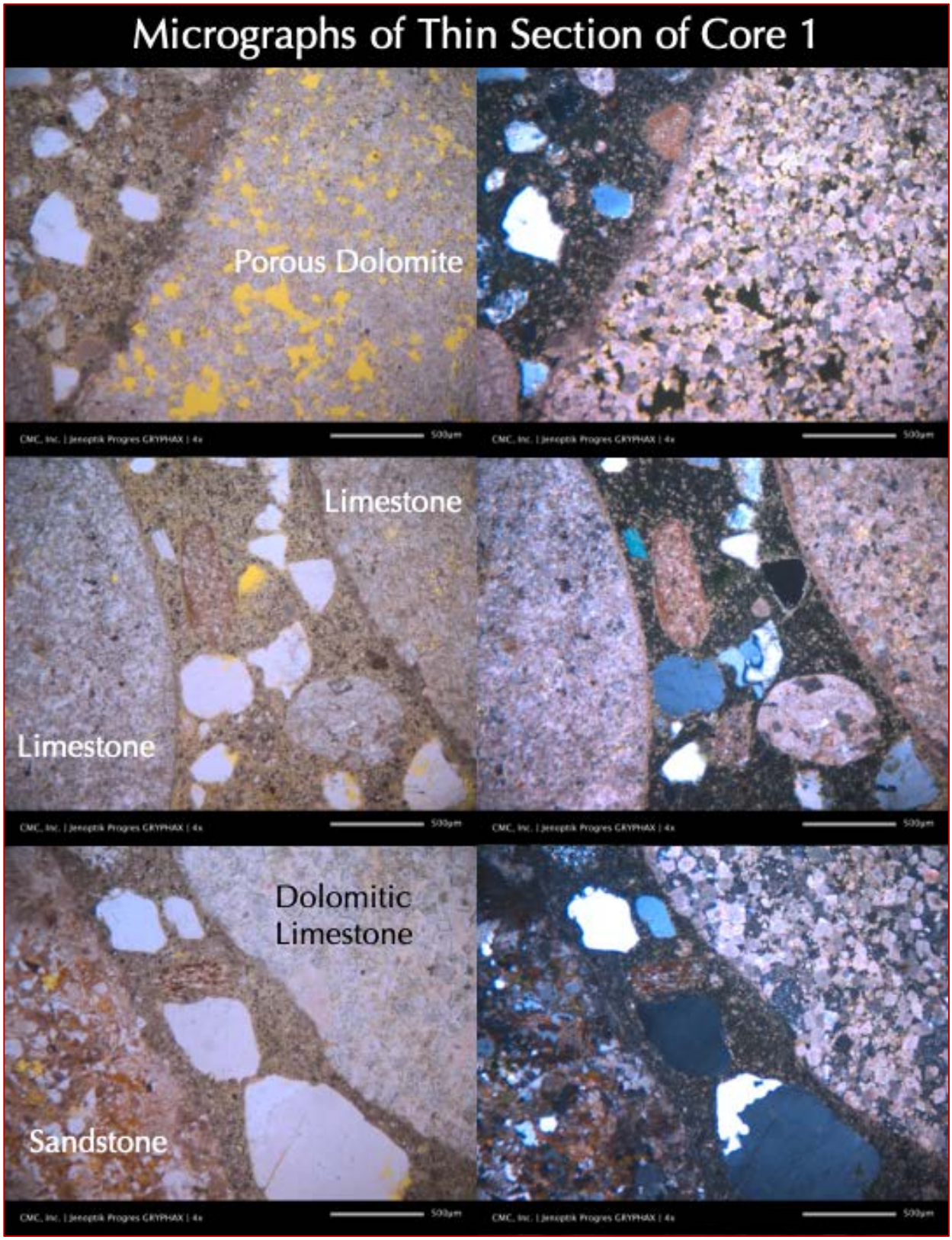

Figure 41: Micrographs of thin section of Core 1 taken with a Nikon Eclipse E600 POL Petrographic microscope with an attached Jenoptik Progres Gryphax camera showing many calcareous gravel particles in coarse aggregate and siliceous-calcareous particles in the interstitial fine aggregate scattered over variably carbonated Portland cement paste.

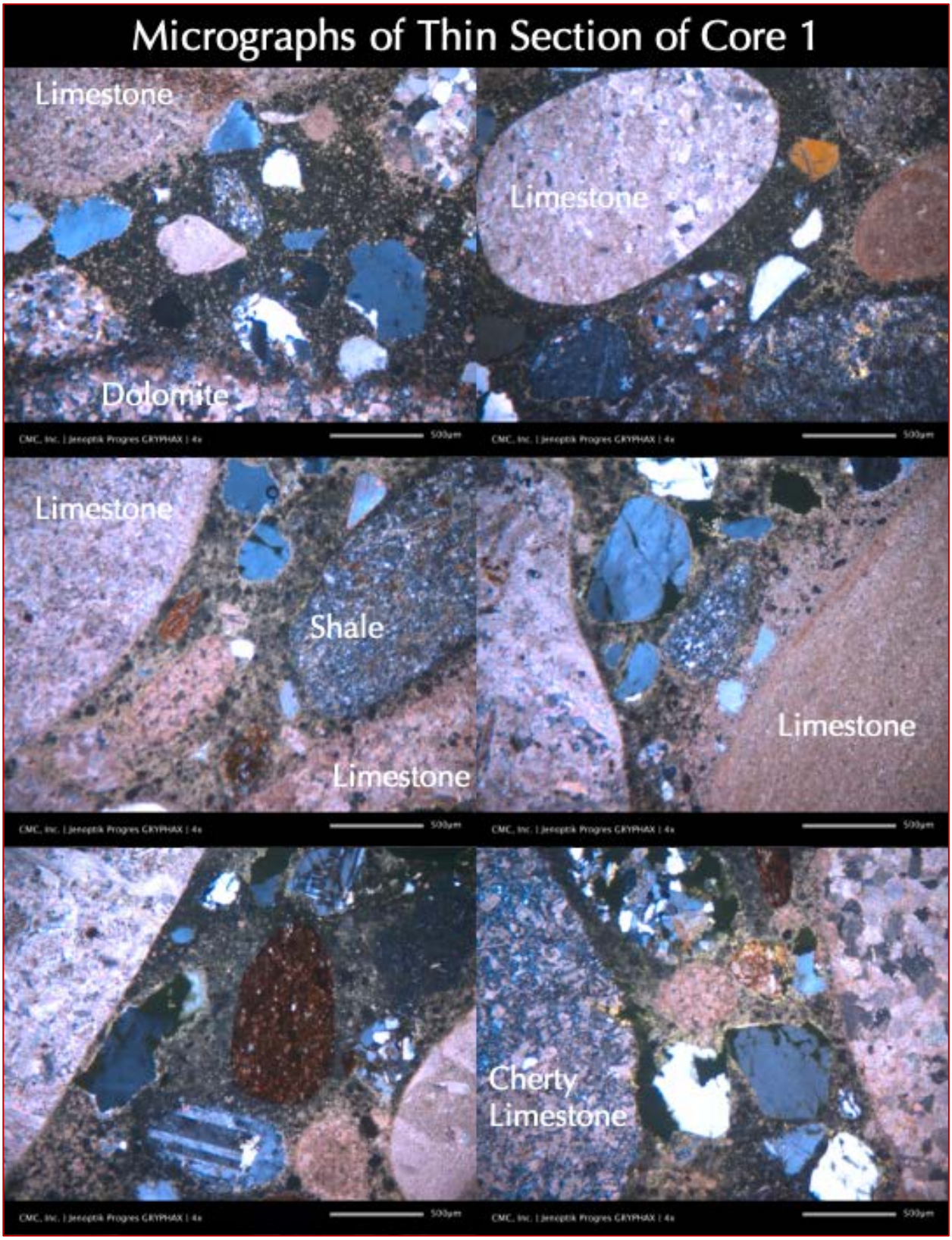

Figure 42: Micrographs of thin section of Core 1 taken with a Nikon Eclipse E600 POL Petrographic microscope with an attached Jenoptik Progres Gryphax camera showing many calcareous gravel particles in coarse aggregate and siliceous-calcareous particles in the interstitial fine aggregate scattered over variably carbonated Portland cement paste.

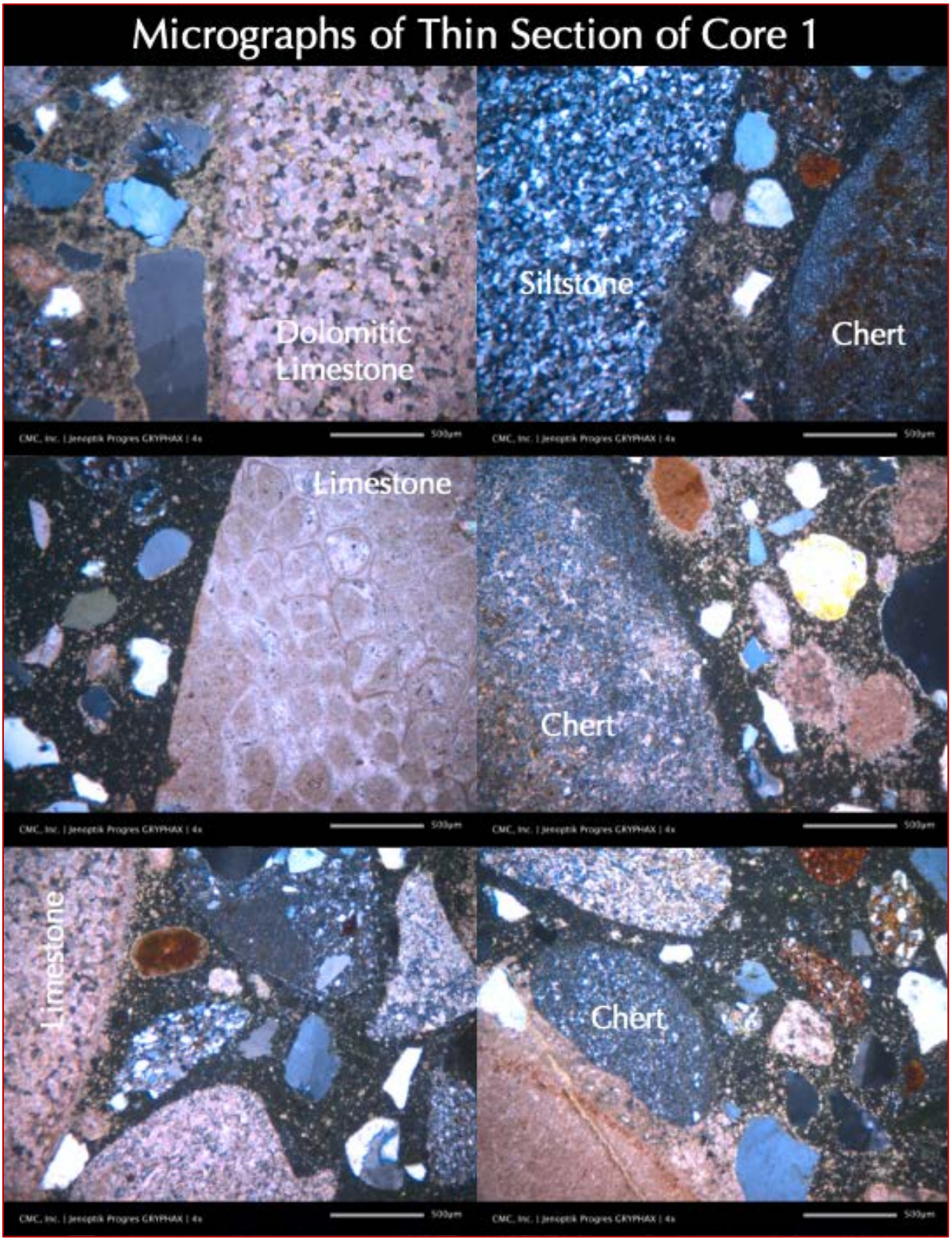

Figure 43: Micrographs of thin section of Core 1 taken with a Nikon Eclipse E600 POL Petrographic microscope with an attached Jenoptik Progres Gryphax camera showing many calcareous gravel particles in coarse aggregate and siliceous-calcareous particles in the interstitial fine aggregate scattered over variably carbonated Portland cement paste.

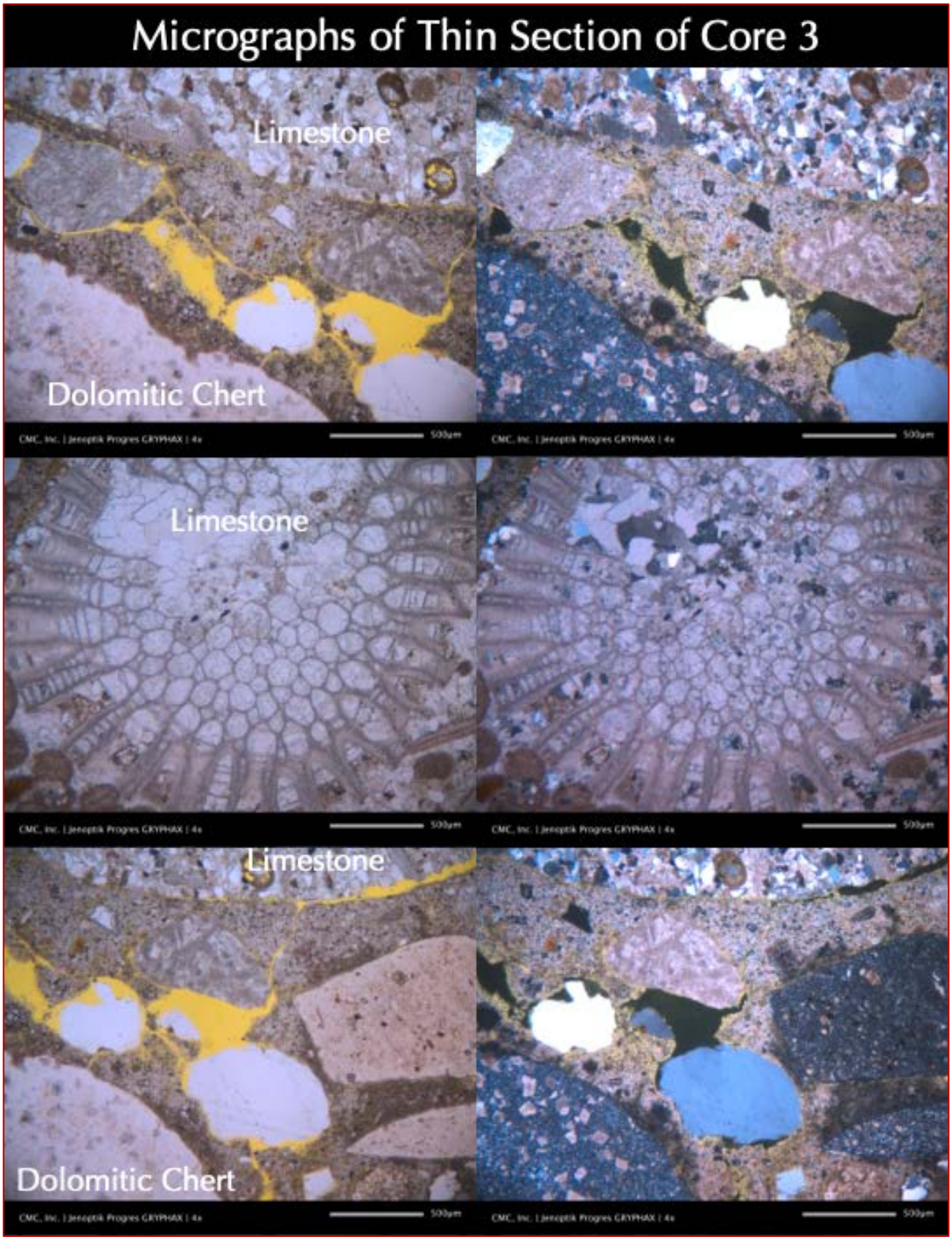

Figure 44: Micrographs of thin section of Core 3 taken with a Nikon Eclipse E600 POL Petrographic microscope with an attached Jenoptik Progres Gryphax camera showing many calcareous gravel particles in coarse aggregate and siliceous-calcareous particles in the interstitial fine aggregate scattered over variably carbonated Portland cement paste.

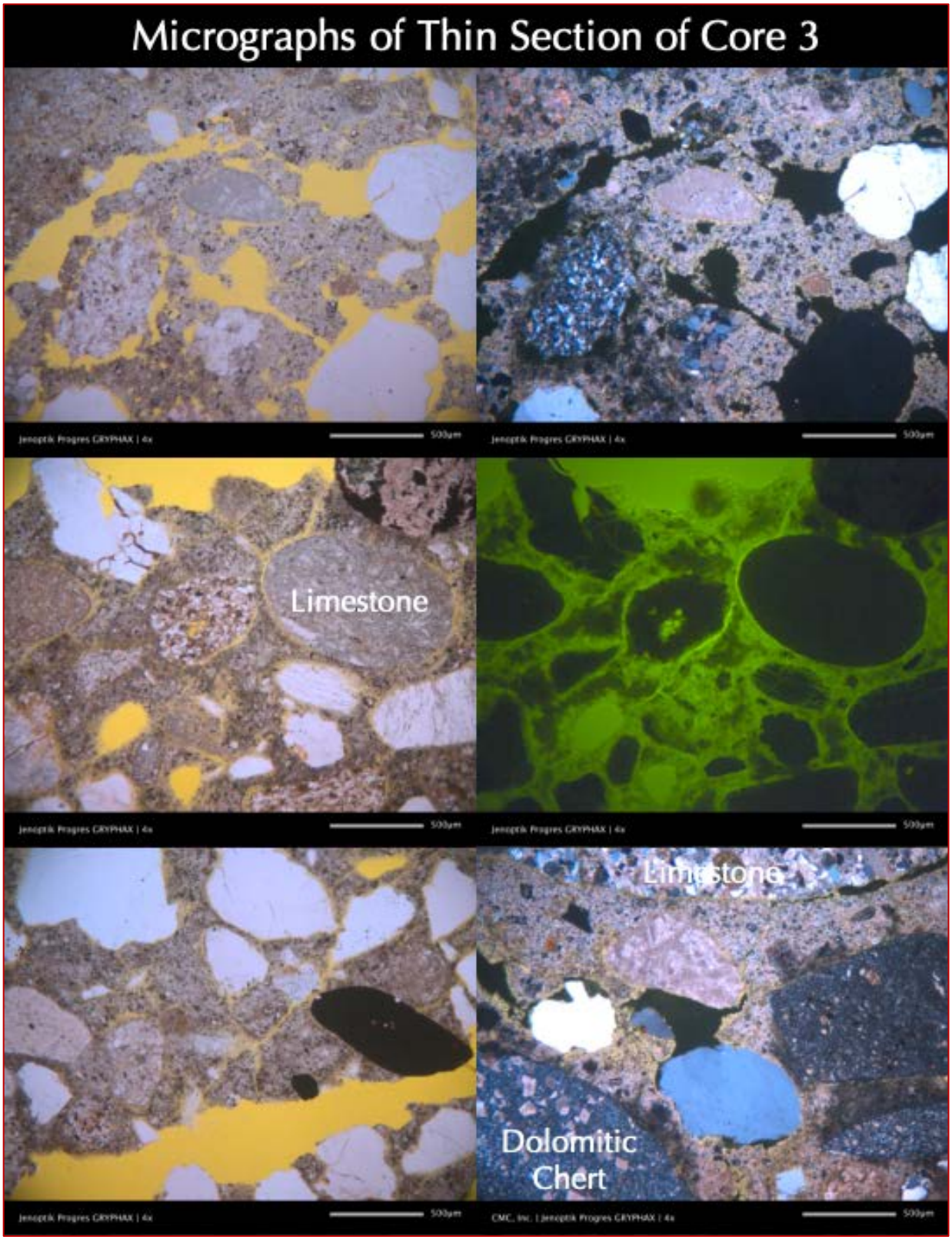

Figure 45: Micrographs of thin section of Core 3 taken with a Nikon Eclipse E600 POL Petrographic microscope with an attached Jenoptik Progres Gryphax camera showing microcracks extending into concrete transecting and circumscribing the aggregate particles. Cracks are highlighted in fluorescent epoxy in plane, crossed, or fluorescent light modes.

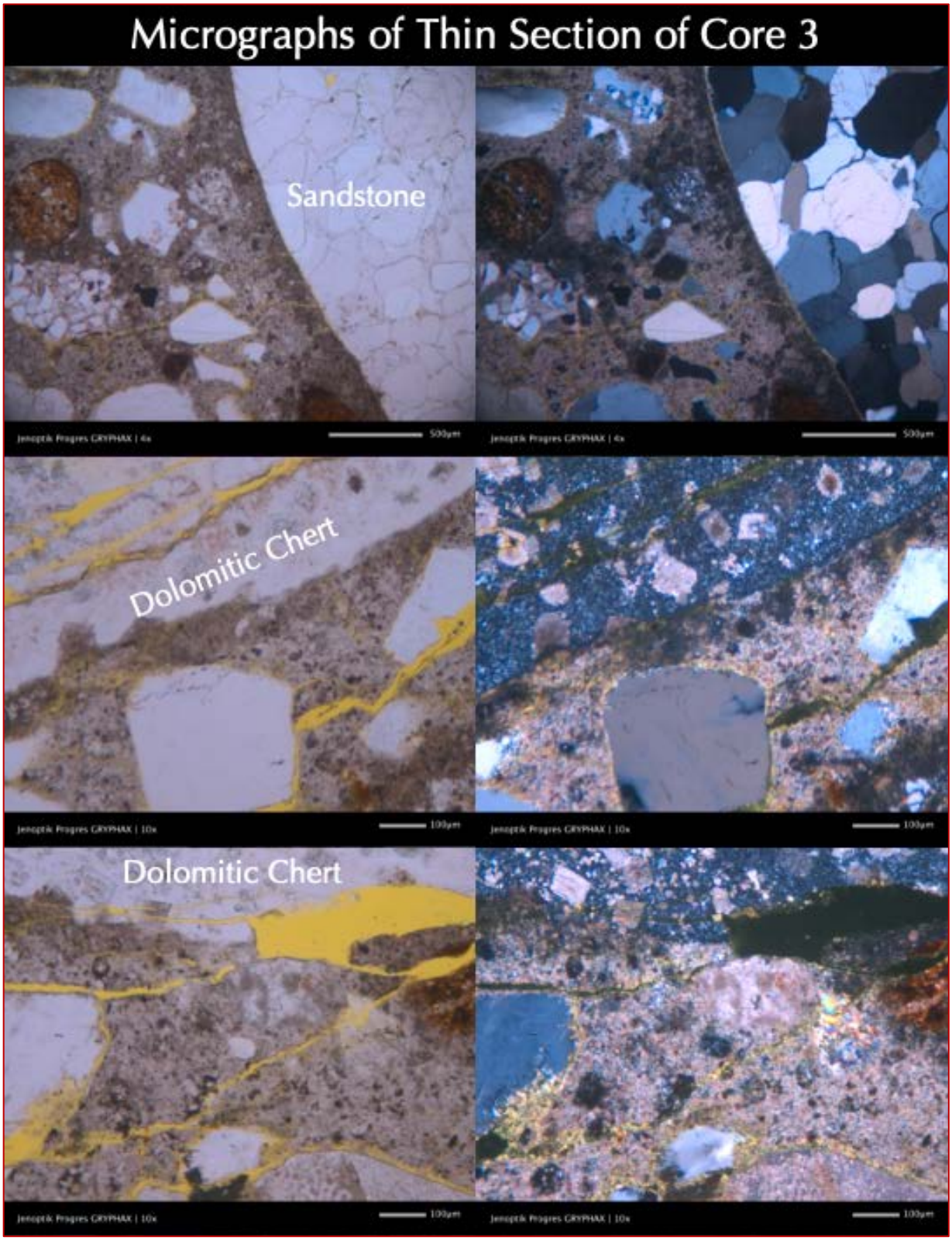

Figure 46: Micrographs of thin section of Core 3 taken with a Nikon Eclipse E600 POL Petrographic microscope with an attached Jenoptik Progres Gryphax camera showing many calcareous gravel particles in coarse aggregate and siliceous-calcareous particles in the interstitial fine aggregate scattered over variably carbonated Portland cement paste.

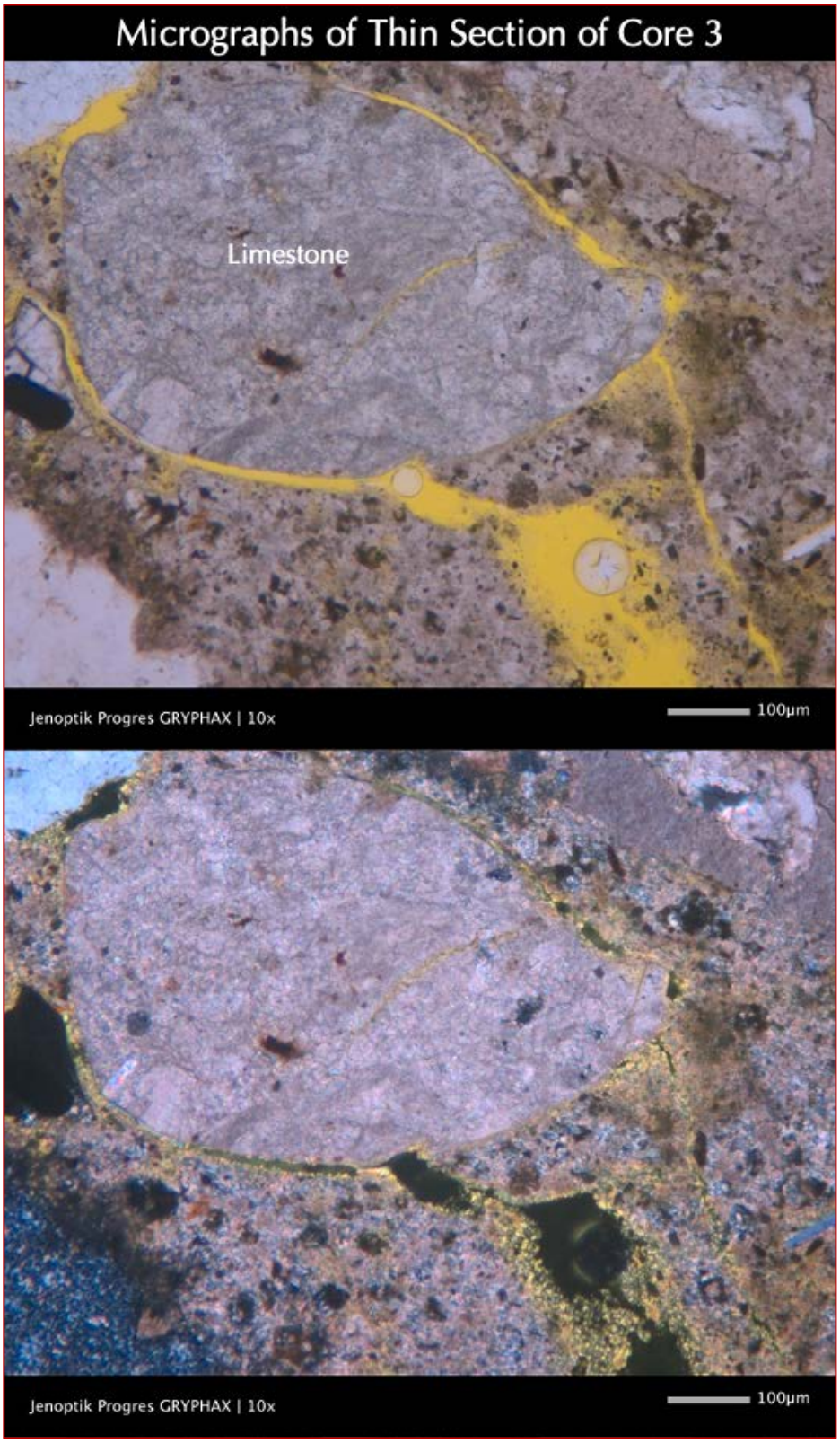

Figure 47: Micrographs of thin section of Core 3 taken with a Nikon Eclipse E600 POL Petrographic microscope with an attached Jenoptik Progres Gryphax camera showing many calcareous gravel particles in coarse aggregate and siliceous-calcareous particles in the interstitial fine aggregate scattered over variably carbonated Portland cement paste.

COARSE AGGREGATES IN CONCRETE

Coarse aggregates are compositionally similar calcareous gravel in all three cores having nominal maximum sizes of 1 inch (25 mm) and containing limestone, dolomite, limestone having microcrystalline to cryptocrystalline silica or chert inclusions, dolomitic chert, fossiliferous limestone (biosparite), and siliceous limestone. Particles are variably dense, variably porous, and variably colored from light to dark gray, brown, red, and other color tones that are characteristic of gravels. Particles are equidimensional to elongated, sub-rounded to well-rounded, unaltered, many show dark weathering and/or reaction rims, and mostly uncracked except the ones along the paths of cracks.

Coarse aggregate particles are well-graded and well-distributed. Many limestone and dolomite particles having microcrystalline silica or chert inclusions show potential reactivity to cement alkalis in the presence of moisture as reaction rims, cracks from reactive particles to paste, and occasional alkali-silica reaction gels inside such cracks. Coarse aggregate particles have been potentially unsound due to such alkali-silica reactions during their service in the concrete and contributed to the extensive cracking seen through the entire depths of Cores 1 and 3.

FINE AGGREGATES IN CONCRETE

Fine aggregates are compositionally similar natural siliceous-calcareous sands in all three samples having nominal maximum sizes of $^{3}/_{8}$ in. (9.5 mm) where siliceous component contains quartz, quartzite, feldspar, chert, granite, sandstone, quartz siltstone and shale, and, calcareous component contains limestone and dolomite of various types mentioned in the calcareous gravel coarse aggregate particles. Particles are variably colored, rounded to subangular, dense, hard, equidimensional to elongated, unaltered, uncoated, and mostly uncracked except the ones along the paths of cracks. Fine aggregate particles are well-graded and well-distributed. There is no evidence of alkali-aggregate reaction of fine aggregate particles although such reaction is possible for many chert particles found in fine aggregate. Fine aggregate particles have been sound during their service in the concrete and did not contribute to the cracking of slab.

The following Table summarizes properties of coarse and fine aggregates in the samples.

Properties and Compositions of Aggregates	Cores 1 and 3
Coarse Aggregates	
Types	Calcareous gravel
Nominal maximum size (in.)	1 inch (25 mm)
Rock Types	Limestone, dolomite, limestone having microcrystalline to cryptocrystalline silica or chert inclusions, dolomitic chert, fossiliferous limestone (biosparite), and siliceous limestone
Angularity, Density, Hardness, Color, Texture, Sphericity	Variably dense, variably porous, and variably colored from light to dark gray, brown, red, and other color tones that are characteristic of gravels

Properties and Compositions of Aggregates	Cores 1 and 3
Cracking, Alteration, Coating	Particles are equidimensional to elongated, sub-rounded to well-rounded, unaltered, many show dark weathering and/or reaction rims, and mostly uncracked except the ones along the paths of cracks.
Grading & Distribution	Well-graded and Well-distributed
Soundness	Unsound due to the presence of alkali-reactive chert inclusions in many limestone particles that have participated in alkali-silica reactions
Alkali-Aggregate Reactivity	Found in limestone and dolomite particles that contain chert inclusions
Fine Aggregates	
Types	Natural siliceous-calcareous sand
Nominal maximum size (in.)	$^{3}/_{8}$ in. (9.5 mm)
Rock Types	Siliceous component contains quartz, quartzite, feldspar, chert, granite, sandstone, quartz siltstone and shale, and, calcareous component contains limestone and dolomite of various types mentioned in the calcareous gravel coarse aggregate particles
Cracking, Alteration, Coating	Variably colored, rounded to subangular, dense, hard, equidimensional to elongated
Grading & Distribution	Well-graded and Well-distributed
Soundness	Sound
Alkali-Aggregate Reactivity	None although the potential exists for particles that contain microcrystalline silica either as separate particles as chert or as inclusions in limestone or dolomite

Table 2: Properties of coarse and fine aggregates of concrete.

PASTE IN CONCRETE

Properties and composition of hardened cement pastes are summarized in Table 2. Pastes are moderately dense, medium gray, uniform in color throughout the depth of concrete. Freshly fractured surfaces have subvitreous lusters and subconchoidal textures. Residual and relict Portland cement particles are present and estimated to constitute 8 to 10 percent of the paste volumes. Besides Portland cement, no other pozzolanic or cementitious materials are found. Hydration of Portland cement is normal in the interior bodies.

Properties and Compositions of Paste	Cores 1 and 3
Color, Hardness, Porosity, Luster	Moderately dense, medium gray, uniform in color throughout the depth of concrete. Freshly fractured surfaces have subvitreous lusters and subconchoidal textures.
Residual Portland Cement Particles	Normal, 8 to 10 percent of the paste volumes
Calcium hydroxide from cement hydration	Normal, 10 to 14 percent by paste volume in the interior
Pozzolans, Slag, etc.	None
Water-cementitious materials ratio (*w/cm*), estimated	0.40 to 0.45
Cement Content (bags per cubic yard)	6 to $6^{1}/_{2}$

Properties and Compositions of Paste	Cores 1 and 3
Secondary Deposits	None
Depth of Carbonation, mm	1 to 2 mm from topping surface but sporadic throughout the interior of concrete
Microcracking	Extensive microcracking from freezing of concrete at saturated conditions, and alkali-silica aggregate reactions
Aggregate-paste Bond	Moderately tight to weak
Bleeding, Tempering	None
Chemical deterioration	Alkali-silica aggregate reaction of potentially reactive cherty limestone and dolomitic chert gravel

Table 3: Proportions and composition of hardened cement pastes.

The textural and compositional features of the pastes are indicative of Portland cement contents estimated to be 6 to 6½ bags per cubic yard, and, water-cement ratios (*w/c*) estimated to be 0.40 to 0.45 in the interior bodies of concrete. Carbonation is 1 to 2 mm from topping surface but sporadic throughout the interior of concrete. Aggregate-paste bonds are moderately tight to weak. Extensive microcracking is present in both cores that are judged to be from freezing of concrete at critically saturated conditions, and alkali-silica aggregate reactions.

AIR

Concrete in both Cores 1 and 3 are non-air-entrained having air contents estimated to be less than 1 percent.

CHLROIDE PROFILES

Results of water-soluble chloride contents determined from potentiometric titration according to the procedures of ASTM C 1218 are given below:

Sample	Chloride Contents from Potentiometric Titration		
	% Chloride by mass of concrete	Cement Content assuming 15 percent	Chloride as percent by mass of *cement* (assuming 15 percent cement in concrete)
Core 1 – Topping	0.0457	0.15	0.304
Core 1 – Concrete Mid-Depth	ND	0.15	-
Core 1 – Concrete Bottom	0.0546	0.15	0.364
Core 3 – Topping	0.0514	0.15	0.342
Core 3 – Concrete Mid-Depth	ND	0.15	-
Core 3 – Concrete Bottom	ND	0.15	-

Table 4: Water-soluble chloride contents from the topping and substrate concrete components of Cores 1 and 3. ND indicates negligible chloride which was not detected by titration.

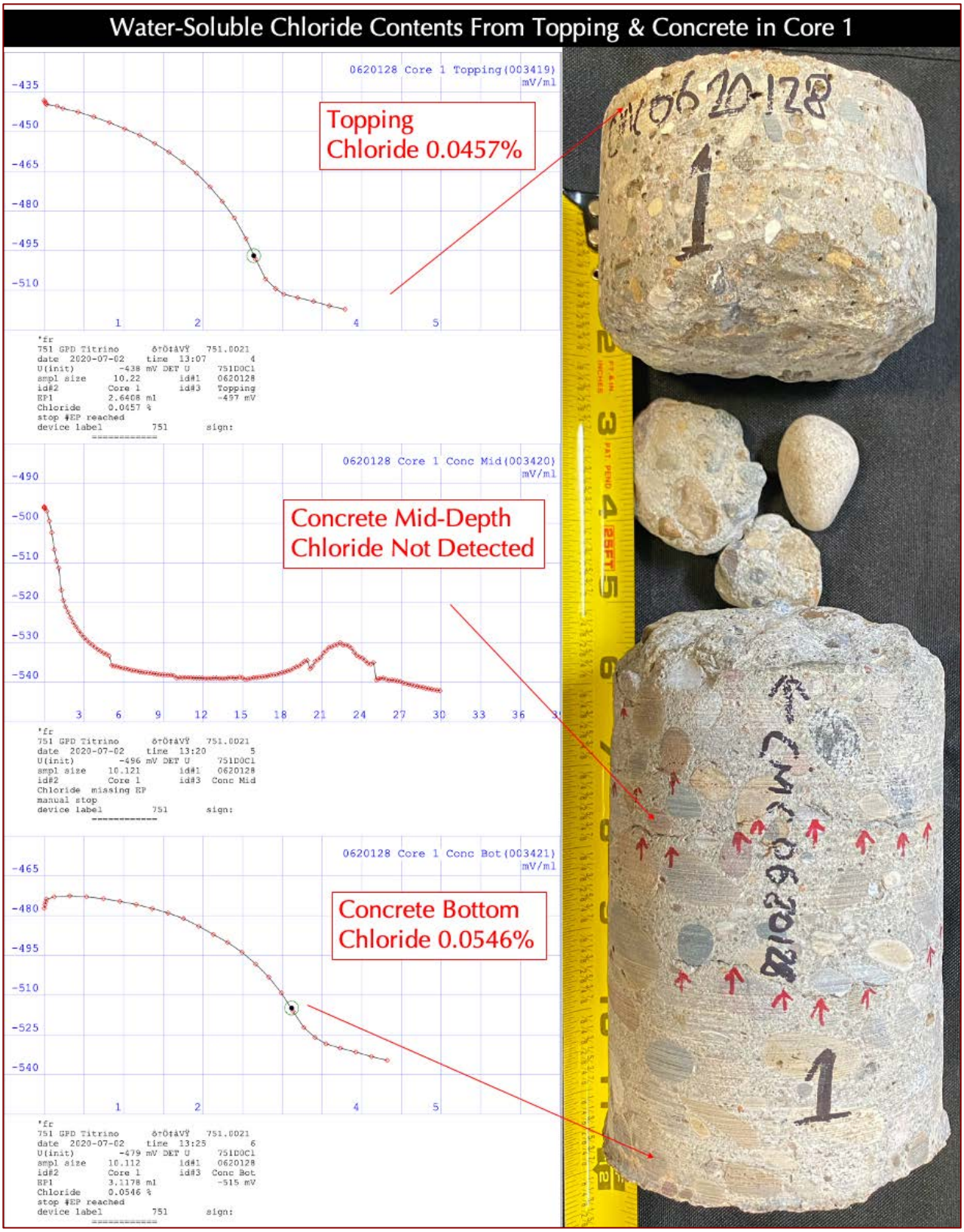

Figure 48: The potentiometric titration curves of chloride analyses where the equivalent points of titration, marked as EP1, represent the steepest points in the curves. Chloride contents are determined from equivalent points times 0.177 divided by sample weight (which is approximately 10.00 grams).

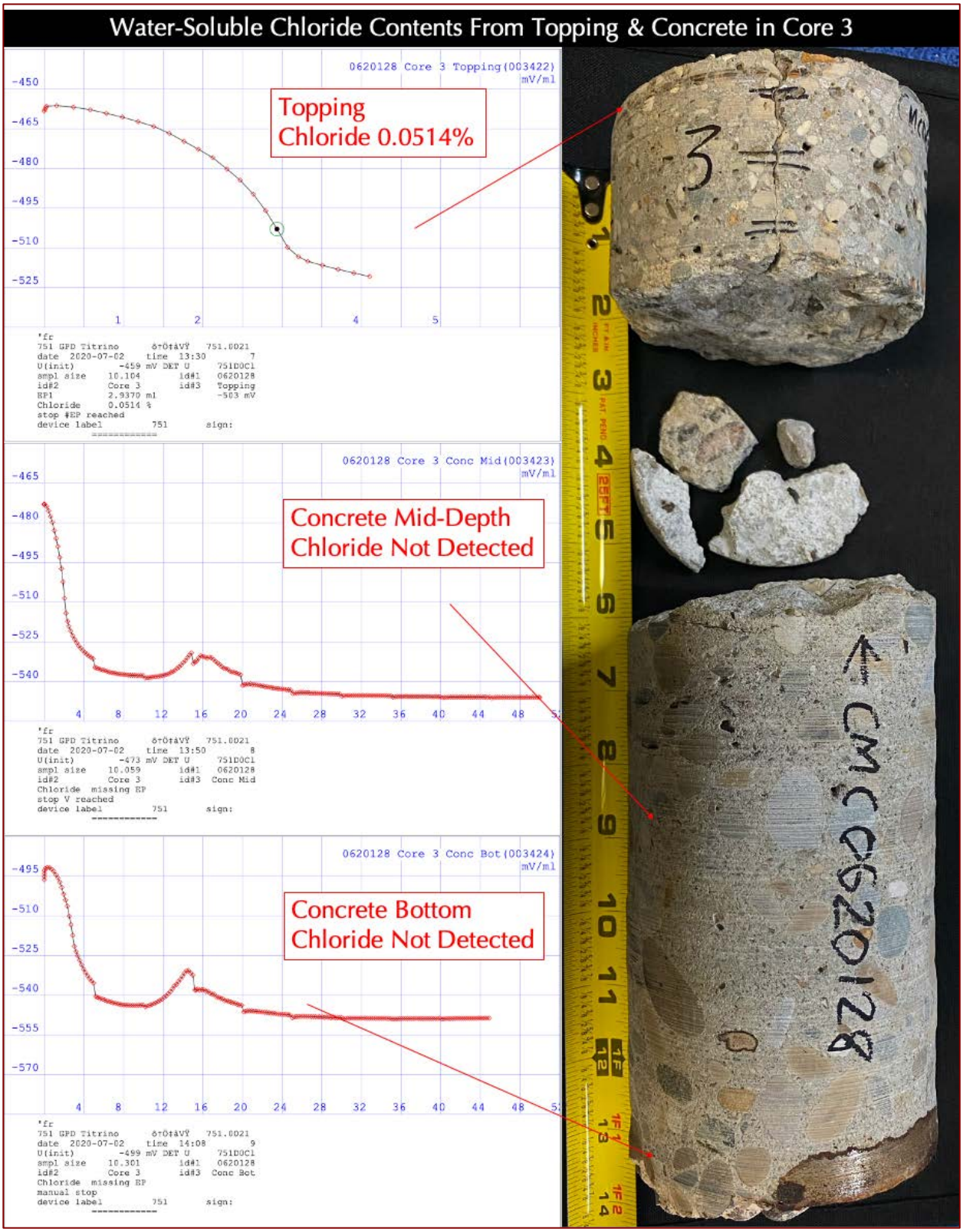

Figure 49: The potentiometric titration curves of chloride analyses where the equivalent points of titration, marked as EP1, represent the steepest points in the curves. Chloride contents are determined from equivalent points times 0.177 divided by sample weight (which is approximately 10.00 grams).

DISCUSSIONS

CRACKING FROM CYCLIC FREEZING AND THAWING OF NON-AIR-ENTRAINED CONCRETE

The non-air-entrained nature of concrete and its exposure to an outdoor environment of cyclic freezing and thawing, and intermittent exposure of water from splashing of pool water have developed an ideal environment for cracking of a non-air-entrained concrete slab around the pool during freezing at critically saturated conditions. The extensive network of cracks oriented parallel to the exposed surface of concrete and extended through the entire depth of slab in both Cores 1 and 2 are the classic testaments of such freezing-induced deterioration of the slab especially due to its prolixity to the pool water.

CRACKING FROM UNSOUND ALKALI-SILICA REACTIVE GRAVEL AGGREGATES

Cracks formed from freezing have opened up channels for migration of moisture deep inside the concrete. The presence of moisture along with high alkalis from Portland cement used during mid-20th century and potentially alkali-silica reactive chert component found in many limestone gravel particles have developed another ideal scenario for distress – alkali-silica reaction. Many reactive cherty limestone and dolomitic chert gravel coarse aggregate particles showed dark reaction rims, cracks extending from reactive gravels to paste, and alkali-silica reaction products inside the cracks – the three tell-tale signatures of distress due to alkali-silica aggregate reactions.

Alkali-silica reaction, however, is found to have played a subordinate role compared to freezing for development of most of the cracks seen in the concrete. It is the freezing-related cracks that have opened up pathways for migration of moisture deep inside the slab to promote alkali-silica reactions. Cracks from alkali-silica reaction have intensified the overall frequency of cracking, no doubt, but the overall surface-parallel orientation of cracks through the entire thickness of slab is most likely formed due to cyclic freezing and thawing of a non-air-entrained concrete at critically saturated conditions.

ROLE OF TOPPING IN PROTECTING UNDERLYING UNSOUND DETERIORATING CONCRETE SUBSTRATE

Unlike extensive through-depth cracking in the concrete substrate, the 2-in. thick topping placed in 1991 is free of any cracks and present in sound and serviceable condition. Most of the distress in concrete slab i.e. freezing-related through-depth cracking is judged to have formed during the service period of 1955 through 1991.

However, topping is not bonded to the underlying deteriorated concrete. In all three cores, the topping was completely de-bonded from the spalled concrete surfaces, where the concrete surface were spalled due to freezing-related cracking. Topping was applied on concrete containing many surface-parallel cracks that have prevented development of a good bond to the newly applied topping.

CARBONATION-INDUCED CORROSION OF REINFORCING STEEL IN CONCRETE

Spalling of the underside of concrete in the suspended top slab of vault and exposed corroded steel reinforcement found in the field photos of underside of the top slab are distresses judged to be due to carbonation-induced corrosion of steel reinforcement situated near the formed bottom end of the top slab. This is evidenced from beige discoloration of concrete found at the bottom end of Core 1, in the fragmented bottom chunk in Core 2, and at the bottom end of Core 3 – all three cores showed such beige discoloration of paste due to carbonation of the underside surface of top slab from carbon dioxide in the ambient air of the vault. Corrosion of steel and associated reddish-brown corrosion products are observed in all three cores situated within this carbonated zone at the underside of top slab. Besides, water-soluble chloride analyses of concrete showed negligible chloride at the bottom end of Core 3 (except at the bottom of Core 1 which showed detectable chloride probably introduced from the pool water during service, probably prior to the installation of topping). The observed corrosion of steel at the underside and associated spalling probably occurred more due to de-passivation of the protective oxide films around steel by reduction in inherent alkalinity of concrete by atmospheric carbonation.

FUTURE DURABILITY AND SERVICEABILITY

In summary, based on detailed petrographic examinations and chloride analyses of cores from around the pool deck, the observed deck slab, which represents the top suspended slab of adjacent underground vault is found to be present in poor deteriorated condition in having extensive through-depth cracking in two of the three cores to complete fragmentation of concrete in the third core. The topping in all three cores are present in sound and serviceable condition, however, with barely any bond to the underlying concrete substrate. Based on extensive cracking and fragmentation, future serviceability of the concrete substrate is judged to be poor, which is preferable to be replaced for long-term durability and serviceability of the pool deck.

REFERENCES

ASTM C 856 “Standard Practice for Petrographic Examination of Hardened Concrete,” Vol. 4.02, ASTM International, West Conshohocken, PA, 2019.

ASTM C 1218 “Standard Test Method for Water-Soluble Chloride in Mortar and Concrete,” Vol. 4.02, ASTM International, West Conshohocken, PA, 2017.

Jana, D., “Sample Preparation Techniques in Petrographic Examinations of Construction Materials: A State-of-the-art Review,” *Proceedings of the 28th Conference on Cement Microscopy*, International Cement Microcopy Association, Denver, Colorado, pp. 23-70, 2006.

✪ ✪ ✪ END OF TEXT ✪ ✪ ✪

END OF REPORT[1]

[1] The CMC logo is made using a lapped polished section of a 1930's concrete from an underground tunnel in the U.S. Capitol.